Chemical Engineering Journal, Volume 482, February 2024, Article number 148826
DOI: 10.1016/j.cej.2024.148826

Simultaneous removal of organic micropollutants and metals from water by a multifunctional β-cyclodextrin polymer-supported-polyaniline composite

Pin Wang [a], Guangyu An [b], Peter Jarvis [c], Wen Liu [d], Shunke Ding [a], Ruixin Qu [a], Zhanghan Li [a], Cheng Ye[a], Wenhai Chu [a, *]

[a] State Key Laboratory of Pollution Control and Resource Reuse, College of Environmental Science and Engineering, Tongji University, Shanghai, 200092, China

[b] State Key Laboratory of Environmental Aquatic Chemistry, Research Center for Eco-Environmental Sciences, Chinese Academy of Sciences, Beijing, 100085, China

[c] Cranfield University, College Road, Cranfield, Bedfordshire MK43 0AL, United Kingdom

[d] College of Environmental Sciences and Engineering, Peking University, Beijing 100871, China

* Corresponding author:

E-mail address: feedwater@126.com

Address: Room 407, National Engineering Research Center for Urban Pollution Control, 1239 Siping Road, Yangpu District, Shanghai, 200092, China

Published by Elsevier. This is the Author Accepted Manuscript issued with: Creative Commons Attribution Non-Commercial No Derivatives License (CC:BY:NC:ND 4.0). The final published version (version of record) is available online at DOI:10.1016/j.cej.2024.148826. Please refer to any applicable publisher terms of use.

Abstract

The occurrence of diverse pollutants in water resources across the globe, including organic micropollutants and heavy metals, has challenged the efficacy of many existing water treatment processes. Various materials and media have been developed for removal of these compounds, but few have the capacity to remove multiple contaminants which are typically present in real water sources. Here we report on a novel sorbent (PANI@PCDP) for the simultaneous removal of organic micropollutants and heavy metals during a single process. Cr(VI) and bisphenol A (BPA) were selected as target pollutants due to their frequent occurrence in aquatic environments and the significant health risks they pose. PANI@PCDP exhibited a high level of performance for removal of BPA and total Cr at pH 6 for initial concentrations of 0.5-100 mg L^{-1} for Cr(VI) and 0.228-22.8 mg L^{-1} for BPA. Up to 98% Cr was removed at pH 6 through the adsorption and reduction of Cr(VI), followed by the sequestration of the generated Cr(III). In addition, BPA could be captured by PANI@PCDP at an adsorption rate of 1.4×10^{-1} g mg^{-1} min^{-1} as a result of the fast formation of complexes with the media. When the PANI@PCDP media was tested on a wider variety of emerging organic micropollutants, including chlorinated aromatic compounds, simple aromatics, and pharmaceuticals, good removal was observed. Such performance benefits arise from the integration of porous β-cyclodextrin polymers with polyaniline, which provides the PANI@PCDP with multiple binding sites for contaminant removal. In addition, the PANI@PCDP can be regenerated at least five times without loss in performance using a facile procedure, providing evidence for its practical application in water treatment.

Keywords

Adsorption, organic micropollutants, heavy metals, Cr(VI), water treatment

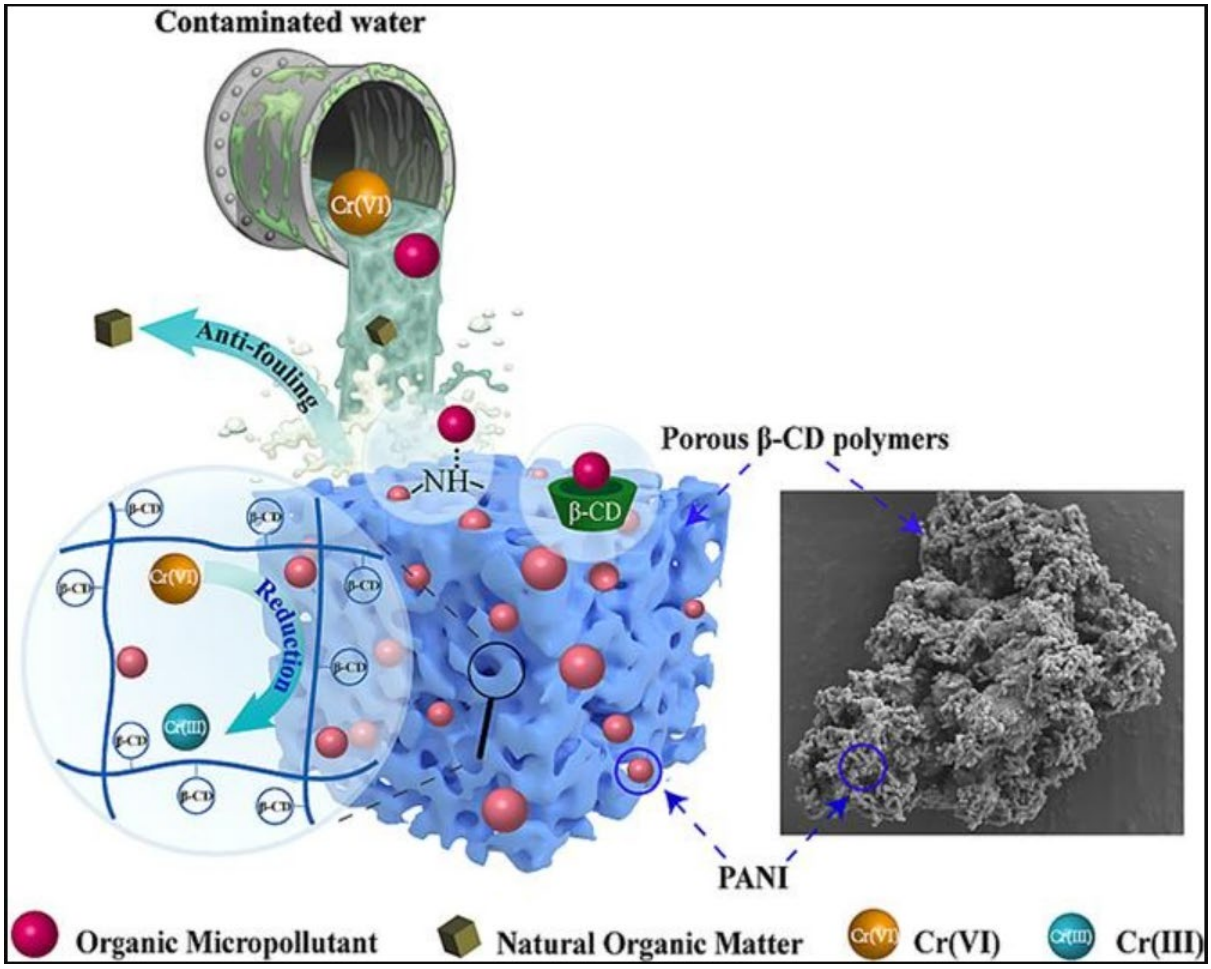
Contaminated water
Cr(VI)
Anti-fouling
NH
β-CD
Porous β-CD polymers
Cr(VI)
Reduction
Cr(III)
PANI
Organic Micropollutant
Natural Organic Matter
Cr(VI)
Cr(III)

1. Introduction

Pollution of water resources from heavy metals and organic micropollutants is widespread across the globe [1–7]. The contamination of natural water resources mainly arises from the unrestricted discharge of industrial effluents and wastewater, both of which pose considerable risks to aquatic ecology and human health [8,9]. Hexavalent chromium (Cr(VI)) is commonly present in the effluents from electroplating, tannery, and paint manufacturing industries, with concentrations ranging up to thousands of milligrams per liter [10–12]. Cr(VI) has been recognized as being carcinogenic and mutagenic [13]. The consumption of Cr(VI)-contaminated water is one of the major exposure pathway to humans, which can cause serious life-threatening diseases such as renal impairment, liver dysfunction, and even lung cancer [14,15]. Bisphenols analogues are chemicals that are largely used during the industrial manufacture of plastic and food/beverage containers [16]. Bisphenol A (BPA) is the most frequently detected species found in aquatic environments at concentrations that range from a few nanograms per liter up to hundreds of micrograms per litre in water [17,18] BPA has been associated with significant human health risks, including prostate cancer [19]. Both Cr(VI) and BPA have been widely detected in river basins such as the Pearl River in China, the Mississippi River in the United States, and the Danube River in Europe [1,2,4–7]. However, conventional water treatment processes exhibit limited efficacy for simultaneous removal of multiple categories of micropollutants. As a result, some recalcitrant micropollutants can end up in treated water.

Significant efforts have been made to develop advanced water treatment technologies to address the issues regarding the combined pollution. However, many water treatment processes targets only a single chemical, or a small group of similar pollutants. For example, reduction-precipitation and ion exchange have applied for Cr(VI) [20,21], and biodegradation and advanced oxidation processes have been used

for BPA removal [22,23]. Adsorption is widely acknowledged as one of the most achievable and reliable techniques for removal of both heavy metals and organic micropollutants from drinking water, municipal sewage, and industrial effluents [24,25]. Activated carbon [26], clay minerals [27], and polymers [28,29] are commonly used as adsorbents for both heavy metals and organic micropollutants. Polyaniline (PANI) has attracted considerable attention with regard to the removal of heavy metals because it has high stability, is non-toxic, is inexpensive to produce and, importantly, has a high affinity towards heavy metals, including Cr(VI) [30–33]. In addition, PANI in the emeraldine salt state contains reduced benzenoid units and oxidized quinoid units [34]. This feature enables the reductive transformation of Cr(VI) to Cr(III) after the adsorption of Cr(VI) to PANI. This process considerably alleviates the environmental risks associated with Cr(VI) toxicity because Cr(III) is 2–3 orders of magnitude lower in toxicity than Cr(VI) and has reduced mobility when compared to the oxidized form [35]. One of the problems associated with using PANI is its propensity to self-aggregate [36]. In turn, this reduces the potential for it to remove pollutants and be recycled [37]. As a result, recent research has focused on the immobilization of PANI inside various substrates to form composite materials. Substrates used include clay [30,38], magnetite nanoparticles [32,39], graphene [40] and polystyrene [33,41]. However, most of these studies have focused on the adsorption and reduction of Cr(VI), while the generated Cr(III) was overlooked. As a result, a high level of total Cr remained in the treated effluent, meaning additional treatment for Cr(III) removal was required in order to meet the water quality objectives (for example, the WHO maximum concentration limit for total Cr in drinking water is 0.05 mg L^{-1} [42]). In addition, these media have not addressed the removal challenge when both metal and organic pollutants are present, as few of these composites have active sites for organic micropollutant capture.

To realize the synchronous removal of micropollutants, an advanced strategy was developed in this study through the anchoring of PANI onto the selected polymer of β-cyclodextrin. Cyclodextrin is a promising adsorbent for the separation of various water contaminants, including endocrine-disrupting chemicals [43–48], dyes [48,49], pesticides [50], and rare earth elements [51]. Recently, Alsbaiee et al. (2016) proposed a type of porous β-cyclodextrin (P-CDP) which contained polymers crosslinked by rigid aromatic structures for eliminating organic micropollutants. Porous polymer materials are considered ideal substrates owing to their tunable chemistry and processable structure [52]. It was therefore hypothesized that the incorporation of PANI into P-CDP would endow the resulting composite with the capacity for simultaneous removal of multiple contaminants from water.

With this in mind, the aim of this study was to develop and test a novel PANI@PCDP media with the intention of targeting both metals and organic micropollutants. Cr(VI) and bisphenol A were selected as target pollutants due to their frequent occurrence in water resources and their significant health risks. The media adsorption performance in removing Cr and BPA was benchmarked against utilization of PANI and P-CDP in isolation. The impacts of pollutant concentrations on the adsorption by PANI@PCDP were assessed over a wide range of pollutant concentrations (0.5-200 mg L^{-1} for Cr(VI) and 0.2–24 mg L^{-1} for BPA). The more general application of this media was assessed by testing against a broader range of emerging organic micropollutants with different physicochemical properties. In addition, the application of PANI@PCDP in practice was evaluated in three types of real water matrices (i.e., surface water, wastewater, tap water) and the recycling of PANI@PCDP was studied.

2. Material and Method

2.1 Reagents

β-cyclodextrin (≥99%), tetrafluoroterephthalonitrile (≥99%), tetrahydrofuran (THF), N,N-dimethylformamide (DMF), 1,5-diphenylcarbazide, K_2CO_3, $CrCl_3 \cdot 6H_2O$, ammonium persulfate, aniline and BPA were purchased from Shanghai Macklin Biochemical Co., Ltd. $K_2Cr_2O_7$ was purchased from Sinopharm Chemical Reagent Co. Ltd., Shanghai, China. All reagents were used as received. Hydrochloric acid solution (0.001−0.1 mol L^{-1}) and sodium hydroxide solution (0.001 mol L^{-1}) were used to adjust the pH of solutions.

2.2 Media Preparation

2.2.1 Synthesis of P-CDP

The synthesis of P-CDP was performed following the method reported by Alsbaiee et al. [28]. A glass regent bottle containing 80 mL of anhydrous THF/DMF (9:1 by volume) equipped with a magnetic stir bar was charged with β-cyclodextrin (2 g), tetrafluoroterephthalonitrile (1 g), and K_2CO_3 (0.3 g). The mixture was bubbled with N_2 for 3 minutes. Then, the N_2 inlet was removed, and the bottle was immediately sealed with a cap. The mixture was placed on a hot stirring plate (85 °C) and stirred at 500 r.p.m. for 2 days. After the orange suspension was cooled and filtered, 1 mol L^{-1} HCl was used to remove the residual K_2CO_3. The yellow solids were recovered and soaked twice in 10 mL of Milli-Q water (18.25 MΩ) for 15 minutes twice in 10 mL of THF for 30 minutes, and once in 15 mL of dichloromethane for 15 minutes. Finally, the solid was soaked in a liquid nitrogen bath for 5 minutes and freeze-dried under a high vacuum for 3 hours. The final light-yellow solid was stored at 4 °C.

2.2.2 Preparation of PANI@PCDP

PANI was synthesized using the chemical oxidation method [34]. A certain amount of P-CDP was dispersed in 80mL of 1 mol L^{-1} HCI under rapid stirring for 30 minutes in a round-bottom flask. 0.5 mL of aniline was added to the flask and stirred constantly at ambient temperature for 3 hours to ensure the complete adsorption of aniline into the P-CDP. Then, 1 mol L^{-1} HCl with 1.254 g of ammonium persulfate was added to the mixture by pumping. The suspension was held in a stirred an ice bath (<2 °C) for 5 hours. The dark-green suspension was filtered, and the recovered dark-green solid was isolated and washed with Milli-Q water (18.25 MΩ) and absolute ethanol until the filtrate became colorless. Finally, the dark-green solid was freeze-dried under a high vacuum overnight. The effect of the PANI/P-CDP mass ratio (mg/mg) on the adsorption performance of the composite was investigated by preparing PANI@PCDP with different ratios of 2:1, 3:1, and 4:1. Preliminary experiments were undertaken to determine the most appropriate mass ratio for further testing. In these experiments, solutions of 52 mg L^{-1} Cr(VI) (equivalent to 1 mmol L^{-1}) and 22.8 mg L^{-1} BPA (equivalent to 0.1 mmol L^{-1}) were used to test solution at a sorbent dose of 1 g L^{-1} at pH 6.0. The removal of Cr(VI) rose as the mass of PANI in the composite increased. However, the adsorption of BPA on the composite decreased when the mass ratio was higher than 3. The PANI@PCDP media with a mass ratio of 3:1 was therefore the preferred choice for all experiments.

2.3 Characterization

The morphology of the sorbents was observed using scanning electron microscopy (Gemini SEM 300, ZEISS, Germany). The functional groups of the sorbents were characterized using Fourier transform infrared spectrometry (FT-IR) (Thermo Scientific Nicolet iS20, USA). The zeta potentials of the sorbents were measured using a laser zeta analyzer (Malvern, Zetasizer ZS90, UK). The elemental chemical

composition states of the sorbents were characterized using X-ray photoelectron spectroscopy (XPS, Thermo Scientific K-Alpha, USA).

2.4 Batch Adsorption Experiments

Adsorption experiments were performed in 30 ml scintillation vials equipped with magnetic stirrer bars. 20 mg of the sorbent was mixed with 20 mL of the pollutant solutions, giving a sorbent dose of 1g L^{-1}. All studies were conducted on a hot plate which controlled water temperature at 25 °C using a stirring rate of 300 rpm.

The adsorption performance of PANI, PCDP and PANI@PCDP was tested with the solution containing Cr(VI) or BPA. To evaluate the impact of pH on the adsorption performance of the sorbents, the pH of test solution was adjusted to 1.0, 2.0, 3.0, 4,0, 5.0 and 6.0. These pH conditions were chosen to prevent precipitation from interfering with the measurement of Cr(III) [33]. The time to reach adsorption equilibrium for Cr(VI) and BPA was 3 hours and 0.5 hours, respectively. The concentration of total Cr was determined using an inductively coupled plasma-optical emission spectrometer (ICP-OES, 5110, Agilent, US). The residual concentrations of Cr(VI) were determined based on the diphenyl carbazide method using a HACH DR6000 UV–vis spectrophotometer (Loveland, US) at 540 nm, and 1,5-diphenylcarbazide was used as the chromogenic reagent [53]. The residual concentrations of Cr(III) were measured using the UV–vis spectrophotometer at 585 nm [33]. The concentration of BPA was measured using high-performance liquid chromatography (HPLC-2010, SHIMAZU, Kyoto, Japan). More details on the HPLC parameters for BPA analysis are provided in Text S1. The data analysis regarding the efficiency of pollutant removal by the sorbents and the resultant adsorption capacity of the sorbents is given in Text S2. The data are reported and presented as the average and standard deviation of three replicates.

Impacts of initial concentrations of Cr and BPA on the adsorption performance of the PANI@PCDP were tested at a sorbent dose of 1g L^{-1} at pH 6.0. The pollutant concentration varied between 0.5 and 100 mg L^{-1} for Cr, and 0.228 and 22.8 mg L^{-1} (equivalent to 0.001 and 0.1 mmol L^{-1}) for BPA.

Adsorption of Cr(III) to sorbents (PANI, PCDP, and PANI@PCDP) was carried out by mixing 50 mg of the sorbent with 50 mL of a solution containing 50 mg L^{-1} of $CrCl_3 \cdot 6H_2O$ at pH 6.0 for 3 hours. The Cr(III) and total Cr were measured after filtration.

The kinetics of adsorption of pollutants onto PANI@PCDP was studied separately at an initial Cr(VI) concentration of 112 mg L^{-1} or BPA concentration of 32 mg $L^{-1}$with a sorbent dose of 1g L^{-1} at pH 6.0 . At time intervals, samples were taken using a syringe followed by filtration through a 0.22 μm membrane filter. Kinetic data were fitted to a pseudo-second-order adsorption mode from Ho and McKay [54] (described in full in Text S3).

Thermodynamic studies of Cr(VI) and BPA adsorption onto PANI@PCDP were conducted using different initial concentrations of the pollutants in the range of 10–200 mg L^{-1} for Cr(VI) or 2.28–31.73 mg L^{-1} (equivalent to 0.01 and 0.139 mmol L^{-1}) for BPA, respectively, with a sorbent dose of 1g L^{-1} at pH 6.0. After the corresponding adsorption time, the suspension was filtered through a 0.22 μm membrane filter. Equilibrium adsorption data were applied to the Langmuir isotherm model (described in Text S4).

In the binary systems (Cr(VI) and BPA spiked together), the initial concentrations of Cr(VI) and BPA were in the range of 30–100 mg L^{-1} for Cr(VI) and 6.8–22.8 mg L^{-1} (0.03–0.1 mmol L^{-1}) for BPA, respectively, at pH 6.0. Tests were carried out following a full factorial design (Table S1). An extended contact time of 6 hours was selected for the binary experiments to achieve equilibrium adsorption. Mono-pollutant adsorption experiments were carried out as control tests.

185 **2.5 Column Adsorption Experiments**

186 Dynamic adsorption experiments were carried out in a column (Ø 12mm × 240 mm) filled with 2.5 mL
187 of PANI@PCDP (0.38 g). Therefore, 1 bed volume was 2.5 mL. The mixed binary solution (10 mg L^{-1}
188 for Cr(VI) and 4.56 mg L^{-1} for BPA, pH 6.0) flowed through the column. The empty bed contact time
189 was 10 min. The analysis of Cr(VI), Cr(III), total Cr, and BPA was performed after filtration.

190 **2.6 PANI@PCDP Recycling Studies**

191 20 mg of pristine sorbent was first mixed with 20 mL of the binary pollutant solution (100 mg L^{-1} for
192 Cr(VI) and 22.8 mg L^{-1} for BPA). After adsorption, the sorbent was collected and regenerated firstly by
193 soaking in 0.1 mol L^{-1} NaOH (20 mL) first, then in 0.5 mol L^{-1} HCl (20 mL) for 3 hours successively,
194 followed by recovery by filtration. After washing with distilled water, the sorbent was rinsed with MeOH
195 (20 mL) for 15 minutes. The adsorption-desorption cycle test was repeated five times.

196 **2.7 Evaluation of Adsorption Performance of PANI@PCDP in Real Water**

197 The PANI@PCDP was then applied in various real water matrices. Tap water was collected from Tongji
198 University (Shanghai, China), surface water was collected from a reservoir in the south of China and
199 treated sewage was collected from the secondary wastewater effluent of a municipal water treatment
200 plant in Shanghai. The characteristics of these real water samples are shown in Table S2. The samples
201 of the real water were spiked with Cr(VI) and BPA from stock solutions. 30 mg of PANI@PCDP was
202 mixed with 30 mL of the real water containing Cr(VI) (50 mg L^{-1}) and BPA (22.8 mg L^{-1}) for 3 hours
203 under rapid stirring at pH 6.0. The analysis of the pollutants was carried out after filtration.

204 **2.8 Adsorption of Anthropogenic Contaminants to PANI@PCDP**

205 The applicability of PANI@PCDP for removal of a wider range of organic micropollutants was assessed
206 by testing against 2,4-dichlorophenol, 2,4,6-trichlorophenol, 2-naphthol, sulfamethoxazole, and

amoxicillin separately. Cu(II) was chosen to represent the heavy metal cation. Adsorption experiments for 2,4-dichlorophenol, 2,4,6-trichlorophenol, 2-naphthol, sulfamethoxazole, and amoxicillin were performed in the same way as these for BPA and Cr(VI) (1 g L^{-1} sorbent, 0.1 mmol L^{-1} organic absorbate, 55 mg L^{-1} Cu(II)), except for sulfamethoxazole (0.04 mmol L^{-1} sorbate) due to its lower water solubility. The concentrations of the organic micropollutants before and after adsorption-filtration were analyzed using a UV–vis spectrophotometer (Table S3). The concentration of Cu(II) was determined using ICP-OES.

3. Results and Discussion

3.1 Synthesis and Characterization of PANI@PCDP

PANI@PCDP was prepared by using a pre-adsorption *in-situ* oxidative polymerization method resulting in β-cyclodextrin becoming crosslinked with rigid aromatic groups. The generated P-CDP was utilized as the substrate to support PANI. Aniline was pre-adsorbed onto the substrate so that the polymerization of aniline occurred both on the surface and in the pores of P-CDP (Fig. 1). Scanning electron microscopy (SEM) images confirmed a coral-like structure of PANI agglomerates (Fig. 1a) and the typical three-dimensional porous structure of P-CDP (Fig. 1b) which has been reported previously [46,55]. For PANI@PCDP, the SEM image shows that PANI was uniformly coated onto the inner pore and the outer surface of P-CDP (Fig. 1c). Thus, the three-dimensional P-CDP acts as the host framework for the support of the PANI. In turn, this largely alleviates the spontaneous agglomeration of PANI, which increases the available active sites on PANI@PCDP. The chemical structures of these three sorbents were verified by FT-IR spectroscopy (Fig. 1d). The FT-IR spectrum of PANI@PCDP exhibits almost all of the characteristic absorbance profiles of PANI and P-CDP, though some signals show attenuation. This was attributed to the interaction between the reagents and the materials during the *in-situ* oxidative

polymerization. These results provide strong evidence for the effective incorporation of PANI into the P-CDP framework and its associated structural integrity [28,32]. Measurement of the media surface charge using zeta potential showed that for PANI@PCDP and PANI, this was dependent on proton concentrations with the point of zero charge at pH 8.8 for PANI@PCDP and 9.1 for PANI (Fig. 1e). This was evidence for the protonation of the amino groups associated with PANI. The P-CDP was negatively charged at all pH values tested. The electrostatic interaction between the positively charged PANI and the negative P-CDP was the main driving force for the incorporation of the polymer onto the host materials. The chemical state of the nitrogen functional group on PANI@PCDP was analyzed using XPS. The N 1s core-level spectrum of PANI@PCDP (Fig. 3d) was deconvoluted into three peaks corresponding to quinonoid imine (=N-), benzenoid amine (-NH-), and the doped imine/amine (N^+) electronic state [56]. The confirmation of the benzenoid amine (-NH-) group in the media was supportive of its ability to be able to convert Cr(VI) to Cr(III) due to its strong reductive capacity [34].

【**Figure 1**】

3.2 Adsorption Performance of PANI@PCDP

To explore the impacts of pH on the adsorption of micropollutants using PANI@PCDP, it was tested alongside PANI and P-CDP in insolation. PANI showed a strong adsorptive affinity for Cr(VI) but an extremely low uptake for BPA (Figs. 2a and 2b), while P-CDP removed most of the BPA but almost no Cr(VI) was adsorbed (Figs. 2c and 2d). In contrast, PANI@PCDP exhibited a high uptake capacity for both BPA and Cr(VI) (Figs. 2e and 2f). The removal of BPA by PANI@PCDP was negatively correlated with the proton concentration, increasing removal from 66% at pH 1.0 to 88% at pH 6.0. It is worth noting that the inclusion complexes associated with the *β*-cyclodextrin polymer are primarily responsible for BPA adsorption [55]. At lower pH, the formation of inclusion complexes was hypothesized to be

negatively impacted when the β-cyclodextrin moieties were in the protonated state. The P-CDP when used in isolation results in marginally higher BPA removal (78%–92%) than was seen for the combined PANI@PCDP sorbent (66%-88%). However, given that the effective mass of β-cyclodextrin in PANI@PCDP was approximately 25% of that in the pure P-CDP systems, the BPA removal observed for the composite media was impressive. In terms of Cr(VI) removal, more than 99% of Cr(VI) was removed by PANI@PCDP in the pH range of 1.0–6.0. This applicable range of pH is significantly wider than that for other reported PANI-based composites [30,31,57,58], clay minerals [13,59] and carbon-based composites, for example, graphene [60,61], and carbon nanotubes [62,63]. Most of these media exhibited efficient adsorption of Cr(VI) under extremely acid conditions (pH 1.0–3.0) but poor removal of Cr(VI) at pH 6.0. The detection of small amounts of Cr(III) in the filtrate verified that the media was able to reduce Cr(VI). The uptake of Cr(III) and total Cr by PANI@PCDP were positively associated with increasing pH. The main species of the residual total Cr was Cr(III), which primarily exists in the form of hydrated cations (i.e., $Cr(OH)^{2+}$, $Cr_2(OH)_2^{4+}$) at pH below 6.0 [61]. As the pH reduces, the protonation of amino groups leads to an overall increase in the positive charge density of the PANI@PCDP, which in turn increases the electrostatic repulsion between PANI@PCDP and Cr(III) cations. Therefore, the maximum sequestration of Cr(III) was achieved at pH 6.0, mainly through its chelation with amine/imine groups on the sorbent [13,32]. Most previous studies on Cr(VI) adsorption have typically adopted acidic conditions (pH 1.0–3.0) for highly efficient removal of Cr(VI). As a result, a large portion of Cr(III) was released back into solution resulting in poor removal of total Cr [31,32,60–62]. In this study, up to 98% of total Cr was removed by PANI@PCDP at pH 6.0 showing that efficient removal of total Cr could be achieved in a single process under mild pH conditions. Although the effective mass of PANI in the combined media (PANI@PCDP) was less than that of the control PANI system (around 75% in

PANI@PCDP), the composite media performed as effectively as PANI for Cr(VI) removal (Figs. 2b and 2f). Taking the adsorption capacity of the sorbents at pH 6 as an example, the adsorption capacity of PANI and PANI@PCDP for Cr(VI) was 54.22 mg g^{-1} and 54.95 mg g^{-1}, respectively. However, when considered on an effective mass of PANI basis, the adsorption capacity of PANI@PCDP was 73.26 mg g^{-1} PANI. This was explained by the immobilization of PANI inside the substrate material, which considerably alleviates the agglomeration of PANI and increases the number of available active sites.

【Figure 2】

Impacts of initial concentration of Cr ($[Cr]_0$) and BPA ($[BPA]_0$) on the adsorption performance of PANI@PCDP were investigated to assess the applicability of this media in various contaminated scenarios (see Fig. 3). Over 99% of Cr(VI) was removed in the $[Cr]_0$ range of 0.5–60 mg L^{-1} at pH 6.0, while the removal decreased to 85% as $[Cr]_0$ rose to 80 mg L^{-1}. For BPA, PANI@PCDP removed more than 99% of BPA in the cases of low $[BPA]_0$ (0.228–2.28 mg L^{-1}) at pH 6.0. As $[BPA]_0$ increased to 22.8 mg L^{-1}, the removal of BPA decreased to 87%. The declining removal of the pollutants at high concentration resulted from the insufficient binding sites on the sorbent. These results suggested that the efficient removal of Cr and BPA using PANI@PCDP is achievable in most environmental-related cases, while a higher dose of PANI@PCDP is needed when treating highly contaminated water.

【Figure 3】

The adsorption kinetics of BPA and Cr(VI) to PANI@PCDP both followed the pseudo-second-order model (see Fig. S1), indicating that the adsorption processes were through chemisorption mechanisms [58,60,64]. The pseudo-second-order rate constant (k_{obs}) for BPA adsorption to PANI@PCDP was 1.4×10^{-1} g mg^{-1} min^{-1}, which was 10 times lower than that was reported for PCDP [28]. This could be associated with the decreased surface area due to the loading of PANI. However, this value was 3-700

295 times higher than that seen for other reported sorbents, including β-cyclodextrin-based sorbents
296 [46,48,65–68] and carbon-based composites [69–72] (shown in Table 1). The uptake of BPA by
297 PANI@PCDP was relatively rapid in the first 10 minutes before gradually approaching equilibrium in
298 the later 20 minutes (Fig. S1a). PANI@PCDP reached nearly 75% of its equilibrium uptake of BPA
299 within one minute. The k_{obs} of Cr(VI) adsorption to PANI@PCDP at pH 6.0 was 8.8×10^{-3} g mg^{-1} min^{-1}
300 (Fig. S1b). It was worth noting that the oxidizing capacity of Cr(VI) and the proton doping degree of
301 PANI could be higher at a lower pH value, where the adsorption and reduction of Cr(VI) using PANI-
302 based sorbents could be improved [33,34]. However, the k_{obs} of Cr(VI) adsorption to PANI@PCDP at
303 pH 6.0 was 6-44 times higher than that reported for other PANI-based sorbents (Table 1), which were
304 determined from experiments undertaken at pH 1.5 or 2 [31,32,73,74], and 2.5-17.6 times higher than
305 that seen for other novel composites [13,60,62,75]. These results demonstrated that the binding sites for
306 both BPA and Cr(VI) of PANI@PCDP were readily accessible.
307 The equilibrium adsorption data for PANI@PCDP fitted the Langmuir model for both the metal and
308 organic pollutant (see Fig. S2), indicating the homogeneous distribution of active adsorption sites on the
309 PANI@PCDP for both BPA and Cr(VI) [58,76]. For Cr(VI), the $q_{max,\,e}$ was 81 mg g^{-1} when considered
310 based on the mass of PANI@PCDP. This value was not as high as the $q_{max,\,e}$ reported in some previous
311 studies, which varied between 100 and 700 mg g^{-1} (shown in Table 2). However, these high $q_{max,\,e}$ values
312 from previous research were determined from adsorption experiments undertaken at pH 1.0-2.0, where
313 Cr(VI) is more easily absorbed and reduced when using the PANI-based sorbents. The maximum
314 adsorption capacity at equilibrium ($q_{max,\,e}$) for BPA was 36 mg g^{-1} for PANI@PCDP, while the equivalent
315 figure for P-CDP was 88 mg g^{-1} [55]. The $q_{max,\,e}$ of PANI@PCDP for BPA was much lower than that
316 reported for other β-cyclodextrin-based sorbents (90-400 mg g^{-1}) [46,48,65–67]. This difference arose

317 from the lower effective mass of *β*-cyclodextrin in the PANI@PCDP in comparison to P-CDP or other
318 sorbents. However, PANI@PCDP reached the equilibrium for BPA and Cr(VI) adsorption within 30
319 mins when compared to other sorbents (Table 2).

320 **3.3 Effects of Binary Systems on Specific Pollutant Uptake**

321 The impact of a binary system on the specific pollutant uptake was investigated using mixed solutions
322 with various $[BPA]_0$ and $[Cr(VI)]_0$ (see Fig. 4). The ratios of the adsorption capacities, R_q, were
323 calculated to represent the effect of the binary system on the specific pollutant uptake (see Fig. S3):

324 $$R_q=\frac{q_{b,i}}{q_{m,i}}$$

325 where $q_{b,i}$ and $q_{m,i}$ are the equilibrium uptake of contaminant *i* in the binary system and mono-component
326 system with the same initial concentration, respectively.

327 An $R_q>1$ indicates enhanced adsorption of contaminant *i* in the presence of coexisting contaminants,
328 while an $R_q<1$ is indicative of the inhibition of adsorption for contaminant *i*. If the coexisting contaminant
329 has no impact on the adsorption of contaminant *i* then R_q is equal to 1 [77]. The uptake of BPA was not
330 affected by the coexistence of Cr(VI) in all tested scenarios owing to the specific complexation between
331 BPA and β-cyclodextrin moieties ($1\leq R_q<1.03$, Fig. 4a and S4a) [76,78–80]. For Cr(VI), the impacts of
332 concurrent BPA depended on both $[Cr(VI)]_0$ and $[BPA]_0$ (Fig. 4b and Fig. S4b). In the case of low
333 $[Cr(VI)]_0$ (for example, 30 and 60 mg L^{-1}), BPA had no effect on Cr(VI) adsorption ($1\leq R_q<1.004$), or
334 for Cr(III) (Fig. 4c) and total Cr (Fig. 4d). For a higher $[Cr(VI)]_0$ of 100 mg L^{-1}, the equilibrium uptake
335 decreased by 15% as the $[BPA]_0$ increased from 0 to 22.8 mg L^{-1}. This shows that the presence of BPA
336 negatively affected the adsorption of Cr(VI) at high $[Cr(VI)]_0$ ($0.85<R_q<1$). A plausible explanation for
337 this being that the adsorption of BPA to PANI@PCDP involves other non-specific interactions such as
338 the formation of hydrogen bonds between the amine groups of PANI@PCDP and the hydroxy groups of

BPA, which in turn induces a steric repulsion effect against Cr(VI) [79,81]. In addition, it is worth noting that the $q_{max,e}$ for Cr(VI) was 81 mg g^{-1} (calculated based on the Langmuir model), meaning that there were insufficient binding sites for adsorption when the $[Cr(VI)]_0$ was 100 mg L^{-1} and the sorbent dose was 1 mg L^{-1}. Thus, the interactions between the BPA and the amine groups intensified the Cr(VI) competition for binding sites, leading to an overall reduction in Cr(VI) uptake. Furthermore, a maximum decline of 24% in the Cr(III) formation was observed in the presence of BPA, while the residual $[Cr_{total}]$ increased by up to 18% as $[BPA]_0$ rose to 22.8 mg L^{-1}, which principally resulted from the decreased adsorption of Cr(VI). These results show that the adsorption of BPA and Cr(VI) to PANI@PCDP were virtually independent of one another at low pollutant concentrations that would be more typical of concentrations observed in environmental systems [82,83]. There was a limited impact of BPA on the adsorption of Cr(VI) at extremely high contaminant concentrations, that would not typically be observed in real polluted water sources or industrial effluents.

【**Figure 4**】

3.4 Versatile Applicability Wider application of PANI@PCDP

3.4.1. Dynamic Adsorption of PANI@PCDP

A column adsorption experiment was performed using a mixed solution of BPA and Cr(VI) at pH 6.0. The breakthrough curves of PANI@PCDP for BPA, Cr(VI), and Cr(III) are shown in Fig. 5a. BPA and Cr(VI) started to be detected in the effluent at 500 and 800 bed volumes (BV), respectively (breakthrough taken as 0.050 mg L^{-1} for Cr(VI) and 0.228 mg L^{-1} for BPA). Hence, the effective treatment volume was 500 BV for the binary system investigated here. In addition, the resulting Cr(III) was completely captured within the filter bed without any leakage throughout the duration of the experiment, indicating that no

361 additional measure would be required for sequestration of the Cr(III) sequestration. This result confirmed
362 the potential of the PANI@PCDP media to water treatment.

363 **3.4.2 Recycling Study of PANI@PCDP**

364 A facile process was used for PANI@PCDP regeneration at ambient temperature (25°C). First, 0.1M
365 NaOH was applied as the desorption agent for Cr(VI), and then 0.1 M HCl was used to desorb Cr(III)
366 and also to regenerate benzenoid amine groups on the sorbent. After washing with distilled water, BPA
367 was easily desorbed from PANI@PCDP by rinsing the composite with MeOH. Five consecutive
368 adsorption-desorption cycles were performed for the binary system with almost no decline in adsorption
369 observed for BPA and Cr(VI) adsorption was observed (Fig. 5b). Some limited detection of Cr(III) was
370 measured in the effluent, reaching a maximum concentration of 1.9 mg L^{-1} after 5 cycles. The mild
371 regeneration process and steady consistent removal performance following regeneration for
372 PANI@PCDP provided good evidence for potential implementation of the novel media.

373 **3.4.3 Adsorption Performance in Real Water**

374 Given the interference of potential competing ions and substances in real water, the selectivity of
375 PANI@PCDP for BPA and Cr(VI) was investigated using real water samples spiked with Cr(VI) and
376 BPA (see Fig. 5c). More than 99% of Cr (VI) was removed from all water samples without Cr(III)
377 remaining in the effluents, indicating the strong selectivity of PANI@PCDP towards Cr(VI).
378 Furthermore, PANI@PCDP removed 88.9%, 86.1%, and 81.5% of BPA from tap water, surface water,
379 and sewage, respectively. The natural organic matter and co-existing ions in tap water and surface water
380 showed no noticeable impacts on the adsorption of BPA. The interior cavity of β-cyclodextrin, with a
381 diameter of 0.78 nm, is considered a natural sieve [84]. As a result, large organic molecules are excluded
382 from the binding sites in the interior cavity of the polymer and thus do not bind with the sorbent media.

This size-exclusive exclusion behavior sets PANI@PCDP apart from the common activated carbon-based adsorbents, which tend to be blocked or fouled by natural organic matter when treating real water. The slight decline in removal efficiency of BPA by PANI@PCDP in wastewater was likely to have been induced by the competition of with other coexisting micropollutants that could access the interior cavity of *β*-cyclodextrin.

3.4.4 Adsorption Performance in Removing Other Contaminants

The potential of the general application of PANI@PCDP was tested against a broader range of organic micropollutants of different molecular size and hydrophobicity (Fig. S5), including chlorinated aromatic compounds, simple aromatics, and pharmaceuticals, as well as another heavy metal (Cu^{2+}) (Fig. 5d). Chlorophenols are widely used in agriculture and industrial production and are considered carcinogens, among which 2,4-dichlorophenol and 2,4,6-trichlorophenol have been detected in groundwater and surface water [85,86]. 2-naphthol was a representative of polycyclic aromatic hydrocarbon contaminants, frequently used as a biomarker for exposure. Sulfamethoxazole and amoxicillin, two of the most commonly used antibiotics, have frequently been detected in the aquatic environment [87,88]. Cu^{2+} is another common heavy metal pollutant detected in aquatic systems [89,90]. Copper contamination is primarily caused by human activities, such as the application in bactericides and animal feed additives, and the metal electroplating industry (Li et al., 2021; Li et al., 2023). Among those organic micropollutants, sulfamethoxazole had the lowest removal efficiency of 60%, while amoxicillin showed the highest removal efficiency of 99%. 85% of 2-naphthol was adsorbed, which was slightly higher than that seen for chlorophenols. Differences in the removal for different compounds might be related to the structure and hydrophobicity of those compounds. The removal of Cu^{2+} was unsatisfying (<50%), indicating limited chelation of the metal with the amine/imine group. This suggests that the synergic

405 effects of electrostatic attraction and chelation enable PANI@PCDP to remove metal anions more
406 effectively than metal cations.

407 【**Figure 5**】

408 **3.5 Adsorption Mechanisms**

409 The superior performance of PANI@PCDP for the simultaneous removal of multiple micropollutants
410 can be explained by the unique structure and the versatile functional groups on the media. A step-by-step
411 strategy was adopted to elucidate the essential mechanisms involved in the adsorption process. The
412 complete adsorption process and the underlying mechanisms are illustrated in Fig. 6.

413 According to the analysis above, the mechanism for the uptake of organic micropollutants by
414 PANI@PCDP followed a multistage process. Firstly, the organic molecules must access the binding sites
415 of the interior cavity, a process that excludes large molecules by size exclusion. This intrinsic size-sieving
416 effect contributes to the efficient removal of micropollutants from real water without fouling by, for
417 example, natural organic matter. Next, the organic substances are partially or entirely anchored in the
418 cavity of *β*-cyclodextrin as a guest molecule, forming host-guest complexes. This process is mainly
419 driven by hydrophobic interactions. The three-dimensional cavities of *β*-cyclodextrin are well-matched
420 with both the planar and non-planar aromatic compounds. In addition, as PANI@PCDP contains a large
421 number of oxygen/nitrogen-containing groups (for example, -OH, -NH_2), hydrogen bonding might also
422 support the adsorption of organics to PANI@PCDP.

423 For Cr(VI) removal, three processes occur when using PANI@PCDP. Firstly, the metal is adsorbed
424 onto the media surface, accompanied by reduction of Cr(VI), before the sequestration of the *in-situ*
425 formed Cr(III). To explore the underlying processes of Cr(VI) adsorption and reduction, the chemical
426 states of N and Cr on the sorbent surface before and after Cr(VI) adsorption at pH 2.0 and pH 6.0 were

analyzed using XPS (see Fig. 7). The appearance of the Cr 2p XPS signal verified the adsorption and reduction of Cr(VI) (Fig. 7a). The signal profiles at the binding energies of 577 eV and 587 eV are assigned to the Cr 2p3/2 orbital and Cr 2p1/2 orbital, respectively, both of which can be deconvoluted into two peaks at two close binding energies, corresponding to Cr(III) and Cr(VI), respectively [93,94]. The higher percentage of Cr(III) on PANI@PCDP at pH 2.0 (compared with that at pH 6.0) can be attributed to the fact that the oxidation capacity of Cr(VI) reduces with decreasing proton concentration (Figs. 7b and 7c) [95]. In addition, the ratio of =N- to -NH- after adsorption at pH 6.0 increased from 0.19 (for the pristine sorbent) to 1.09, indicating that -NH- was oxidized to =N- after reduction of Cr(VI). This ratio rose to 1.77 after Cr(VI) adsorption at pH 2.0 owing to the enhancement of the Cr(VI) oxidation potential under acidic conditions (Figs. 7d-f). Moreover, in comparison to the PANI alone, the PANI@PCDP exhibited higher uptake and reduction capacity for Cr(VI) when considered on an effective mass of PANI basis. This can be attributed to the structure of this composite, where the immobilization of the PANI inside the substrate material considerably alleviates its agglomeration, leading to an increase in the frequency of binding sites for Cr(VI). With respect to the process of Cr(III) adsorption, the adsorption capacity of these sorbents for Cr(III) was tested using $CrCl_3 \cdot 6H_2O$ solution at pH 6.0 as treatment targets. The Cr(III) uptake followed the order of PANI@PCDP (3 mg g^{-1}) ≈ PANI (3.2 mg g^{-1}) < P-CDP (15 mg g^{-1}) (Fig. S6). According to the concentrations of Cr(VI) and Cr(III) in the effluent and the Cr species distribution on the PANI@PCDP after adsorption process (Figs. 2f and 7c), it was estimated that the adsorption capacity of PANI@PCDP for the Cr(III) generated from the reduction of Cr(VI) was 36.6 mg g^{-1}. This result suggests that Cr(III) generated from the redox reaction between Cr(VI) and -NH- can immediately chelate *in situ* with imine groups instead of being released into the bulk solution where it may reach a high level of hydration [96]. Furthermore, the higher uptake of *in situ*

449 formed Cr(III) by PANI@PCDP (compared to the bulky PANI alone) indicates the possibility of there
450 being a negatively charged environment in the inner structure of PANI@PCDP, given that the internal
451 framework of the P-CDP might still carry negative charges as a result of confinement [37]. This would
452 then contribute to the electrostatic attraction between the *in situ* formed Cr(III) cations and the media
453 framework. Based on the analysis above, the overall process begins with the adsorption of Cr(VI). The
454 subsequent reduction of Cr(VI) was the rate-limiting step for Cr(III) sequestration because a small
455 portion of Cr(VI) remained on PANI@PCDP at equilibrium.

456 【**Figure 6**】

457

458 【**Figure 7**】

459 **4. Conclusions**

460 In summary, this work developed a novel composite sorbent, PANI@PCDP, based on low-cost aniline
461 and β-cyclodextrin. PANI@PCDP exhibited excellent versatility in removing multi-contaminants in one
462 single process. Such performance benefits arise from the integration of porous β-cyclodextrin polymers
463 with PANI, which provides PANI@PCDP with multiple binding sites for contaminant removal. PANI
464 plays a major role in the adsorption and reduction of Cr(VI), while the P-CDP host material not only
465 supports the PANI but also plays an essential role in the adsorption of organic micropollutants. The
466 synergistic effects enable the PANI@PCDP to remove Cr(VI) and organic micropollutants
467 simultaneously with high efficacy, affinity, and kinetics under conditions relevant to water purification.
468 Furthermore, PANI@PCDP maintains excellent performance in real matrices (for example, surface water
469 and wastewater) and can be recycled over five times using a facile approach with no loss in performance.
470 Therefore, PANI@PCDP has great potential for addressing complex contamination in aquatic

environments.

Acknowledgements

This work was funded by the National Natural Science Foundation of China (52325001 and 52170009), the National Key Research and Development Program of China (2021YFC3200700 and 2021YFC3200702), Shanghai Science International Cooperation Project (20230714100), and the Fundamental Research Funds for the Central Universities.

Reference

[1] I. Jarić, Ž. Višnjić-Jeftić, G. Cvijanović, Z. Gačić, L. Jovanović, S. Skorić, M. Lenhardt, Determination of differential heavy metal and trace element accumulation in liver, gills, intestine and muscle of sterlet (Acipenser ruthenus) from the Danube River in Serbia by ICP-OES, Microchemical Journal. 98 (2011) 77–81. https://doi.org/https://doi.org/10.1016/j.microc.2010.11.008.

[2] J.-L. Zhao, G.-G. Ying, L. Wang, J.-F. Yang, X.-B. Yang, L.-H. Yang, X. Li, Determination of phenolic endocrine disrupting chemicals and acidic pharmaceuticals in surface water of the Pearl Rivers in South China by gas chromatography–negative chemical ionization–mass spectrometry, Science of The Total Environment. 407 (2009) 962–974. https://doi.org/https://doi.org/10.1016/j.scitotenv.2008.09.048.

[3] Z.Y. Zhao, J.D. Gu, X.J. Fan, H.B. Li, Molecular size distribution of dissolved organic matter in water of the Pearl River and trihalomethane formation characteristics with chlorine and chlorine dioxide treatments, J Hazard Mater. 134 (2006) 60–66. https://doi.org/10.1016/j.jhazmat.2005.10.032.

[4] J. Wang, X. Lu, Q. Jing, B. Zhang, J. Ye, H. Zhang, Z. Xiao, J. Zhang, Spatiotemporal characterization of heavy metal and antibiotics in the Pearl River Basin and pollutants removal assessment using invasive species-derived biochars, J Hazard Mater. 454 (2023) 131409. https://doi.org/https://doi.org/10.1016/j.jhazmat.2023.131409.

[5] L.B. Barber, J.E. Loyo-Rosales, C.P. Rice, T.A. Minarik, A.K. Oskouie, Endocrine disrupting alkylphenolic chemicals and other contaminants in wastewater treatment plant effluents, urban streams, and fish in the Great Lakes and Upper Mississippi River Regions, Science of The Total Environment. 517 (2015) 195–206. https://doi.org/https://doi.org/10.1016/j.scitotenv.2015.02.035.

[6] P. Ho, M.J. Shim, S.D. Howden, A.M. Shiller, Temporal and spatial distributions of nutrients and trace elements (Ba, Cs, Cr, Fe, Mn, Mo, U, V and Re) in Mississippi coastal waters: Influence of hypoxia, submarine groundwater discharge, and episodic events, Cont Shelf Res. 175 (2019) 53–69. https://doi.org/https://doi.org/10.1016/j.csr.2019.01.013.

[7] K. Ng, N. Alygizakis, M.-C. Nika, A. Galani, P. Oswald, M. Oswaldova, Ľ. Čirka, U. Kunkel, A. Macherius, M. Sengl, G. Mariani, S. Tavazzi, H. Skejo, B.M. Gawlik, N.S. Thomaidis, J. Slobodnik, Wide-scope target screening characterization of legacy and emerging contaminants in the Danube River Basin by liquid and gas chromatography coupled with high-resolution mass spectrometry, Water Res. 230 (2023) 119539. https://doi.org/https://doi.org/10.1016/j.watres.2022.119539.

[8] Z. Yan, H. Yang, H. Dong, B. Ma, H. Sun, T. Pan, R. Jiang, R. Zhou, J. Shen, J. Liu, G. Lu, Occurrence and ecological risk assessment of organic micropollutants in the lower reaches of the Yangtze River, China: A case study of water diversion, Environmental Pollution. 239

(2018) 223–232. https://doi.org/10.1016/j.envpol.2018.04.023.

[9] A.C. Johnson, R.L. Donnachie, J.P. Sumpter, M.D. Jürgens, C. Moeckel, M.G. Pereira, An alternative approach to risk rank chemicals on the threat they pose to the aquatic environment, Science of the Total Environment. 599–600 (2017) 1372–1381. https://doi.org/10.1016/j.scitotenv.2017.05.039.

[10] Piyush Malaviya, Asha Singh, Physicochemical Technologies for Remediation of Chromium-Containing Waters and Wastewaters, Crit Rev Environ Sci Technol. 41 (2011) 1111–1172.

[11] R.T. Kapoor, M.F. Bani Mfarrej, P. Alam, J. Rinklebe, P. Ahmad, Accumulation of chromium in plants and its repercussion in animals and humans, Environmental Pollution. 301 (2022). https://doi.org/10.1016/j.envpol.2022.119044.

[12] L. Aljerf, High-efficiency extraction of bromocresol purple dye and heavy metals as chromium from industrial effluent by adsorption onto a modified surface of zeolite: Kinetics and equilibrium study, J Environ Manage. 225 (2018) 120–132. https://doi.org/10.1016/j.jenvman.2018.07.048.

[13] Y. Xu, J. Chen, R. Chen, P. Yu, S. Guo, X. Wang, Adsorption and reduction of chromium(VI) from aqueous solution using polypyrrole/calcium rectorite composite adsorbent, Water Res. 160 (2019) 148–157. https://doi.org/10.1016/j.watres.2019.05.055.

[14] Z. Jin, X. Wang, Y. Sun, Y. Ai, X. Wang, Adsorption of 4-n-Nonylphenol and Bisphenol-A on Magnetic Reduced Graphene Oxides: A Combined Experimental and Theoretical Studies, Environ Sci Technol. 49 (2015) 9168–9175. https://doi.org/10.1021/acs.est.5b02022.

[15] R.T. Kapoor, M.F. Bani Mfarrej, P. Alam, J. Rinklebe, P. Ahmad, Accumulation of chromium

in plants and its repercussion in animals and humans, Environmental Pollution. 301 (2022). https://doi.org/10.1016/j.envpol.2022.119044.

[16] J. Liu, L. Zhang, G. Lu, R. Jiang, Z. Yan, Y. Li, Occurrence, toxicity and ecological risk of Bisphenol A analogues in aquatic environment – A review, Ecotoxicol Environ Saf. 208 (2021). https://doi.org/10.1016/j.ecoenv.2020.111481.

[17] Y. Hu, Q. Zhu, X. Yan, C. Liao, G. Jiang, Occurrence, fate and risk assessment of BPA and its substituents in wastewater treatment plant: A review, Environ Res. 178 (2019) 108732. https://doi.org/10.1016/J.ENVRES.2019.108732.

[18] A.H. Zainuddin, M.Q.J. Roslan, M.R. Razak, F.M. Yusoff, D.E.M. Haron, A.Z. Aris, Occurrence, distribution, and ecological risk of bisphenol analogues in marine ecosystem of urbanized coast and estuary, Mar Pollut Bull. 192 (2023) 115019. https://doi.org/10.1016/J.MARPOLBUL.2023.115019.

[19] B. Borrell, Toxicology: The big test for bisphenol A, Nature. 464 (2010) 1122–1124. https://doi.org/10.1038/4641122a.

[20] Z. Shao, C. Huang, Q. Wu, Y. Zhao, W. Xu, Y. Liu, J. Dang, H. Hou, Ion exchange collaborating coordination substitution: More efficient Cr(VI) removal performance of a water-stable CuII-MOF material, J Hazard Mater. 378 (2019). https://doi.org/10.1016/j.jhazmat.2019.05.112.

[21] Bihuang Xie, Chao Shan, Zhe Xu, Xuchun Li, Xiaolin Zhang, Jiajia Chen, Bingcai Pan, One-step removal of Cr(VI) at alkaline pH by UV/sulfite process: Reduction to Cr(III) and in situ Cr(III) precipitation, Chemical Engineering Journal. 308 (2017) 791–797.

[22] G. Zhou, Y. Cao, Y. Jin, C. Wang, Y. Wang, C. Hua, S. Wu, Novel selective adsorption and

558 photodegradation of BPA by molecularly imprinted sulfur doped nano-titanium dioxide, J
559 Clean Prod. 274 (2020). https://doi.org/10.1016/j.jclepro.2020.122929.
560 [23] J. Xiong, T. An, G. Li, P. Peng, Accelerated biodegradation of BPA in water-sediment
561 microcosms with Bacillus sp. GZB and the associated bacterial community structure,
562 Chemosphere. 184 (2017) 120–126. https://doi.org/10.1016/j.chemosphere.2017.05.163.
563 [24] P.J.J. Alvarez, C.K. Chan, M. Elimelech, N.J. Halas, D. Villagrán, enhance water security,
564 Nat Nanotechnol. 13 (2018). https://doi.org/10.1038/s41565-018-0203-2.
565 [25] S.S. Kerur, S. Bandekar, M.S. Hanagadakar, S.S. Nandi, G.M. Ratnamala, P.G. Hegde,
566 Removal of hexavalent Chromium-Industry treated water and Wastewater: A review, Mater
567 Today Proc. 42 (2020) 1112–1121. https://doi.org/10.1016/j.matpr.2020.12.492.
568 [26] M. Raninga, A. Mudgal, V.K. Patel, J. Patel, M. Kumar Sinha, Modification of activated
569 carbon-based adsorbent for removal of industrial dyes and heavy metals: A review, Mater
570 Today Proc. 77 (2023) 286–294. https://doi.org/10.1016/J.MATPR.2022.11.358.
571 [27] G.G. Hacıosmanoğlu, C. Mejías, J. Martín, J.L. Santos, I. Aparicio, E. Alonso, Antibiotic
572 adsorption by natural and modified clay minerals as designer adsorbents for wastewater
573 treatment: A comprehensive review, J Environ Manage. 317 (2022) 115397.
574 https://doi.org/10.1016/J.JENVMAN.2022.115397.
575 [28] A. Alsbaiee, B.J. Smith, L. Xiao, Y. Ling, D.E. Helbling, W.R. Dichtel, Rapid removal of
576 organic micropollutants from water by a porous β-cyclodextrin polymer, Nature. 529 (2016)
577 190–194. https://doi.org/10.1038/nature16185.
578 [29] S. Jadoun, J.P. Fuentes, B.F. Urbano, J. Yáñez, A review on adsorption of heavy metals from
579 wastewater using conducting polymer-based materials, J Environ Chem Eng. 11 (2023)

109226. https://doi.org/10.1016/J.JECE.2022.109226.

[30] T. Zhou, C. Li, H. Jin, Y. Lian, W. Han, Effective Adsorption/Reduction of Cr(VI) Oxyanion by Halloysite@Polyaniline Hybrid Nanotubes, ACS Appl Mater Interfaces. 9 (2017) 6030–6043. https://doi.org/10.1021/acsami.6b14079.

[31] S. Das, P. Chakraborty, R. Ghosh, S. Paul, S. Mondal, A. Panja, A.K. Nandi, Folic Acid-Polyaniline Hybrid Hydrogel for Adsorption/Reduction of Chromium(VI) and Selective Adsorption of Anionic Dye from Water, ACS Sustain Chem Eng. 5 (2017) 9325–9337. https://doi.org/10.1021/acssuschemeng.7b02342.

[32] A.E. Chávez-Guajardo, J.C. Medina-Llamas, L. Maqueira, C.A.S. Andrade, K.G.B. Alves, C.P. de Melo, Efficient removal of Cr (VI) and Cu (II) ions from aqueous media by use of polypyrrole/maghemite and polyaniline/maghemite magnetic nanocomposites, Chemical Engineering Journal. 281 (2015) 826–836. https://doi.org/10.1016/j.cej.2015.07.008.

[33] J. Ding, L. Pu, Y. Wang, B. Wu, A. Yu, X. Zhang, B. Pan, Q. Zhang, G. Gao, Adsorption and Reduction of Cr(VI) Together with Cr(III) Sequestration by Polyaniline Confined in Pores of Polystyrene Beads, Environ Sci Technol. 52 (2018) 12602–12611. https://doi.org/10.1021/acs.est.8b02566.

[34] J.Y. Shimano, A.G. MacDiarmid, Polyaniline, a dynamic block copolymer: Key to attaining its intrinsic conductivity, Synth Met. 123 (2001) 251–262. https://doi.org/10.1016/S0379-6779(01)00293-4.

[35] M. Costa, Potential hazards of hexavalent chromate in our drinking water, Toxicol Appl Pharmacol. 188 (2003) 1–5. https://doi.org/https://doi.org/10.1016/S0041-008X(03)00011-5.

602 [36] D. Li, R.B. Kaner, Shape and Aggregation Control of Nanoparticles: Not Shaken, Not
603 Stirred, J Am Chem Soc. 128 (2006) 968–975. https://doi.org/10.1021/ja056609n.
604 [37] J. Qian, X. Gao, B. Pan, Nanoconfinement-Mediated Water Treatment: From Fundamental
605 to Application, Environ Sci Technol. 54 (2020) 8509–8526.
606 https://doi.org/10.1021/acs.est.0c01065.
607 [38] A. Olad, F. Farshi Azhar, A study on the adsorption of chromium (VI) from aqueous
608 solutions on the alginate-montmorillonite/polyaniline nanocomposite, Desalination Water
609 Treat. 52 (2014) 2548–2559. https://doi.org/10.1080/19443994.2013.794711.
610 [39] K. Zhu, C. Chen, H. Xu, Y. Gao, X. Tan, A. Alsaedi, T. Hayat, Cr(VI) Reduction and
611 Immobilization by Core-Double-Shell Structured Magnetic Polydopamine@Zeolitic
612 Idazolate Frameworks-8 Microspheres, ACS Sustain Chem Eng. 5 (2017) 6795–6802.
613 https://doi.org/10.1021/acssuschemeng.7b01036.
614 [40] Q. Ji, D. Yu, G. Zhang, H. Lan, H. Liu, J. Qu, Microfluidic Flow through Polyaniline
615 Supported by Lamellar-Structured Graphene for Mass-Transfer-Enhanced Electrocatalytic
616 Reduction of Hexavalent Chromium, Environ Sci Technol. 49 (2015) 13534–13541.
617 https://doi.org/10.1021/acs.est.5b03314.
618 [41] J.J. Alcaraz-Espinoza, A.E. Chávez-Guajardo, J.C. Medina-Llamas, C.A.S. Andrade, C.P.
619 De Melo, Hierarchical composite polyaniline-(Electrospun Polystyrene) fibers applied to
620 heavy metal remediation, ACS Appl Mater Interfaces. 7 (2015) 7231–7240.
621 https://doi.org/10.1021/acsami.5b00326.
622 [42] WHO, Guidelines for Drinking-Water Quality:Fourth Edition Incorporating the First
623 Addendum, in: Geneva, 2017.

[43] M.J. Klemes, Y. Ling, M. Chiapasco, A. Alsbaiee, D.E. Helbling, W.R. Dichtel, Phenolation of cyclodextrin polymers controls their lead and organic micropollutant adsorption, Chem Sci. 9 (2018) 8883–8889. https://doi.org/10.1039/c8sc03267j.

[44] E. García-Díaz, D. Zhang, Y. Li, R. Verduzco, P.J.J. Alvarez, TiO_2 microspheres with cross-linked cyclodextrin coating exhibit improved stability and sustained photocatalytic degradation of bisphenol A in secondary effluent, Water Res. 183 (2020) 116095. https://doi.org/10.1016/j.watres.2020.116095.

[45] Y. Tu, G. Xu, L. Jiang, X. Hu, J. Xu, X. Xie, A. Li, Amphiphilic hyper-crosslinked porous cyclodextrin polymer with high specific surface area for rapid removal of organic micropollutants, Chemical Engineering Journal. 382 (2020) 123015. https://doi.org/10.1016/j.cej.2019.123015.

[46] Z. Sun, L. Zhao, C. Liu, Y. Zhen, W. Zhang, J. Ma, A novel 3D adsorbent of reduced graphene oxide-B-cyclodextrin aerogel coupled hardness with softness for efficient removal of bisphenol A, Chemical Engineering Journal. 372 (2019) 896–904. https://doi.org/10.1016/j.cej.2019.04.217.

[47] D. Zhang, C. Lee, H. Javed, P. Yu, J.H. Kim, P.J.J. Alvarez, Easily Recoverable, Micrometer-Sized TiO 2 Hierarchical Spheres Decorated with Cyclodextrin for Enhanced Photocatalytic Degradation of Organic Micropollutants, Environ Sci Technol. 52 (2018) 12402–12411. https://doi.org/10.1021/acs.est.8b04301.

[48] Y. Zhou, Y. Hu, W. Huang, G. Cheng, C. Cui, J. Lu, A novel amphoteric B-cyclodextrin-based adsorbent for simultaneous removal of cationic/anionic dyes and bisphenol A, Chemical Engineering Journal. 341 (2018) 47–57. https://doi.org/10.1016/j.cej.2018.01.155.

[49] F. Zhao, E. Repo, D. Yin, Y. Meng, S. Jafari, M. Sillanpää, EDTA-Cross-Linked β-Cyclodextrin: An Environmentally Friendly Bifunctional Adsorbent for Simultaneous Adsorption of Metals and Cationic Dyes, Environ Sci Technol. 49 (2015) 10570–10580. https://doi.org/10.1021/acs.est.5b02227.

[50] H. Liu, X. Cai, Y. Wang, J. Chen, Adsorption mechanism-based screening of cyclodextrin polymers for adsorption and separation of pesticides from water, Water Res. 45 (2011) 3499–3511. https://doi.org/10.1016/j.watres.2011.04.004.

[51] F. Nkinahamira, A. Alsbaiee, Q. Zeng, Y. Li, Y. Zhang, M. Feng, C.P. Yu, Q. Sun, Selective and fast recovery of rare earth elements from industrial wastewater by porous β-cyclodextrin and magnetic β-cyclodextrin polymers, Water Res. 181 (2020) 115857. https://doi.org/10.1016/j.watres.2020.115857.

[52] J. Qian, X. Gao, B. Pan, Nanoconfinement-Mediated Water Treatment: From Fundamental to Application, Environ Sci Technol. 54 (2020) 8509–8526. https://doi.org/10.1021/acs.est.0c01065.

[53] X. Wang, N. Chen, L. Zhang, Enhanced Cr(VI) immobilization on goethite derived from an extremely acidic environment, Environ Sci Nano. 6 (2019) 2185–2194. https://doi.org/10.1039/c9en00277d.

[54] E.D. Revellame, D.L. Fortela, W. Sharp, R. Hernandez, M.E. Zappi, Adsorption kinetic modeling using pseudo-first order and pseudo-second order rate laws: A review, Clean Eng Technol. 1 (2020) 100032. https://doi.org/10.1016/J.CLET.2020.100032.

[55] A. Alsbaiee, B.J. Smith, L. Xiao, Y. Ling, D.E. Helbling, W.R. Dichtel, Rapid removal of organic micropollutants from water by a porous β-cyclodextrin polymer, Nature. 529 (2016)

190–194. https://doi.org/10.1038/nature16185.

[56] Y. Xu, J. Chen, R. Chen, P. Yu, S. Guo, X. Wang, Adsorption and reduction of chromium(VI) from aqueous solution using polypyrrole/calcium rectorite composite adsorbent, Water Res. 160 (2019) 148–157. https://doi.org/10.1016/j.watres.2019.05.055.

[57] M. Laabd, A. Imgharn, A. Hsini, Y. Naciri, M. Mobarak, S. Szunerits, R. Boukherroub, A. Albourine, Efficient detoxification of Cr(VI)-containing effluents by sequential adsorption and reduction using a novel cysteine-doped PANi@faujasite composite: Experimental study supported by advanced statistical physics prediction, J Hazard Mater. 422 (2022). https://doi.org/10.1016/j.jhazmat.2021.126857.

[58] A.E. Chávez-Guajardo, J.C. Medina-Llamas, L. Maqueira, C.A.S. Andrade, K.G.B. Alves, C.P. de Melo, Efficient removal of Cr (VI) and Cu (II) ions from aqueous media by use of polypyrrole/maghemite and polyaniline/maghemite magnetic nanocomposites, Chemical Engineering Journal. 281 (2015) 826–836. https://doi.org/10.1016/j.cej.2015.07.008.

[59] A. El-Kordy, A. Elgamouz, A.A. Alrashdi, A. Kali, A. Abdelhamid, A.N. Kawde, N. Tijani, Development and characterization of a clay-HDTMABr composite for the removal of Cr(VI) from aqueous solutions with special emphasis on the electrochemical interface, Arabian Journal of Chemistry. 16 (2023). https://doi.org/10.1016/j.arabjc.2023.105027.

[60] Y. Sun, F. Yu, L. Li, J. Ma, Adsorption-reduction synergistic effect for rapid removal of Cr (VI) ions on superelastic NH2-graphene sponge, Chemical Engineering Journal. 421 (2021) 129933. https://doi.org/10.1016/j.cej.2021.129933.

[61] H. Wang, Y.G. Liu, G.M. Zeng, X.J. Hu, X. Hu, T.T. Li, H.Y. Li, Y.Q. Wang, L.H. Jiang, Grafting of β-cyclodextrin to magnetic graphene oxide via ethylenediamine and application

for Cr(VI) removal, Carbohydr Polym. 113 (2014) 166–173. https://doi.org/10.1016/j.carbpol.2014.07.014.

[62] M. Bhaumik, S. Agarwal, V.K. Gupta, A. Maity, Enhanced removal of Cr(VI) from aqueous solutions using polypyrrole wrapped oxidized MWCNTs nanocomposites adsorbent, J Colloid Interface Sci. 470 (2016) 257–267. https://doi.org/10.1016/j.jcis.2016.02.054.

[63] L. Chen, N. Chen, H. Wu, W. Li, Z. Fang, Z. Xu, X. Qian, Flexible design of carbon nanotubes grown on carbon nanofibers by PECVD for enhanced Cr(VI) adsorption capacity, Sep Purif Technol. 207 (2018) 406–415. https://doi.org/10.1016/j.seppur.2018.06.065.

[64] N. Li, L. Yang, D. Wang, C. Tang, W. Deng, Z. Wang, High-Capacity Amidoxime-Functionalized β-Cyclodextrin/Graphene Aerogel for Selective Uranium Capture, Environ Sci Technol. 55 (2021) 9181–9188. https://doi.org/10.1021/acs.est.0c08743.

[65] J. Li, J. Wang, X. Yuan, Z. Wang, S. Sun, Q. Lyu, S. Hu, Efficient adsorption of BPA and Pb2+ by sulfhydryl-rich β-cyclodextrin polymers, Sep Purif Technol. 309 (2023). https://doi.org/10.1016/j.seppur.2022.122913.

[66] L. Zhou, Q. Huang, H. Ji, X. Tang, Y. Zhang, K. Chai, Efficient adsorption of bisphenol A from water by a hierarchically porous hyper-crosslinked polymer containing β-cyclodextrin polyurethane, Sep Purif Technol. 319 (2023). https://doi.org/10.1016/j.seppur.2023.124076.

[67] M. Usman, A. Ahmed, Z. Ji, B. Yu, Y. Shen, H. Cong, Environmentally friendly fabrication of new β-Cyclodextrin/ZrO2 nanocomposite for simultaneous removal of Pb(II) and BPA from water, Science of the Total Environment. 784 (2021). https://doi.org/10.1016/j.scitotenv.2021.147207.

[68] N. Łukasik, S. Wikarska, H. Świątek, M. Łapiński, T. Klimczuk, K. Hemine, The influence

712 of magnetic particle incorporation on bisphenol A removal by β-cyclodextrin-derived
713 sorbent, Chemosphere. 338 (2023). https://doi.org/10.1016/j.chemosphere.2023.139538.
714 [69] P. Shao, J. Pei, H. Tang, S. Yu, L. Yang, H. Shi, K. Yu, K. Zhang, X. Luo, Defect-rich porous
715 carbon with anti-interference capability for adsorption of bisphenol A via long-range
716 hydrophobic interaction synergized with short-range dispersion force, J Hazard Mater. 403
717 (2021) 123705. https://doi.org/https://doi.org/10.1016/j.jhazmat.2020.123705.
718 [70] Y. Zhao, C. Feng, C. Tian, Z. Li, Y. Yang, Enhanced adsorption selectivity of bisphenol
719 analogues by tuning the functional groups of covalent organic frameworks (COFs), Sep
720 Purif Technol. 297 (2022) 121489.
721 https://doi.org/https://doi.org/10.1016/j.seppur.2022.121489.
722 [71] Z. Fang, Y. Hu, X. Wu, Y. Qin, J. Cheng, Y. Chen, P. Tan, H. Li, A novel magnesium ascorbyl
723 phosphate graphene-based monolith and its superior adsorption capability for bisphenol A,
724 Chemical Engineering Journal. 334 (2018) 948–956.
725 https://doi.org/10.1016/j.cej.2017.10.067.
726 [72] R. Jin, C. Zhao, Y. Song, X. Qiu, C. Li, Y. Zhao, Competitive adsorption of sulfamethoxazole
727 and bisphenol A on magnetic biochar: Mechanism and site energy distribution,
728 Environmental Pollution. 329 (2023). https://doi.org/10.1016/j.envpol.2023.121662.
729 [73] M. Laabd, A. Imgharn, A. Hsini, Y. Naciri, M. Mobarak, S. Szunerits, R. Boukherroub, A.
730 Albourine, Efficient detoxification of Cr(VI)-containing effluents by sequential adsorption
731 and reduction using a novel cysteine-doped PANi@faujasite composite: Experimental study
732 supported by advanced statistical physics prediction, J Hazard Mater. 422 (2022).
733 https://doi.org/10.1016/j.jhazmat.2021.126857.

[74] A. Hsini, Y. Naciri, M. Laabd, A. Bouziani, J.A. Navío, F. Puga, R. Boukherroub, R. Lakhmiri, A. Albourine, Development of a novel PANI@WO_3 hybrid composite and its application as a promising adsorbent for Cr(VI) ions removal, J Environ Chem Eng. 9 (2021). https://doi.org/10.1016/j.jece.2021.105885.

[75] U.O. Aigbe, R. Das, W.H. Ho, V. Srinivasu, A. Maity, A novel method for removal of Cr(VI) using polypyrrole magnetic nanocomposite in the presence of unsteady magnetic fields, Sep Purif Technol. 194 (2018) 377–387. https://doi.org/10.1016/j.seppur.2017.11.057.

[76] Y. Zhou, Y. Hu, W. Huang, G. Cheng, C. Cui, J. Lu, A novel amphoteric B-cyclodextrin-based adsorbent for simultaneous removal of cationic/anionic dyes and bisphenol A, Chemical Engineering Journal. 341 (2018) 47–57. https://doi.org/10.1016/j.cej.2018.01.155.

[77] J.-H. Deng, X.-R. Zhang, G.-M. Zeng, J.-L. Gong, Q.-Y. Niu, J. Liang, Simultaneous removal of Cd(II) and ionic dyes from aqueous solution using magnetic graphene oxide nanocomposite as an adsorbent, Chemical Engineering Journal. 226 (2013) 189–200. https://doi.org/https://doi.org/10.1016/j.cej.2013.04.045.

[78] S. Kundu, N. Korin Manor, A. Radian, Iron-Montmorillonite-Cyclodextrin Composites as Recyclable Sorbent Catalysts for the Adsorption and Surface Oxidation of Organic Pollutants, ACS Appl Mater Interfaces. 12 (2020) 52873–52887. https://doi.org/10.1021/acsami.0c17510.

[79] Z. Sun, L. Zhao, C. Liu, Y. Zhen, W. Zhang, J. Ma, A novel 3D adsorbent of reduced graphene oxide-B-cyclodextrin aerogel coupled hardness with softness for efficient removal of bisphenol A, Chemical Engineering Journal. 372 (2019) 896–904. https://doi.org/10.1016/j.cej.2019.04.217.

[80] K. V. Ragavan, N.K. Rastogi, β-Cyclodextrin capped graphene-magnetite nanocomposite for selective adsorption of Bisphenol-A, Carbohydr Polym. 168 (2017) 129–137. https://doi.org/10.1016/j.carbpol.2017.03.045.

[81] Y. Lv, J. Ma, K. Liu, Y. Jiang, G. Yang, Y. Liu, C. Lin, X. Ye, Y. Shi, M. Liu, L. Chen, Rapid elimination of trace bisphenol pollutants with porous β-cyclodextrin modified cellulose nanofibrous membrane in water: adsorption behavior and mechanism, J Hazard Mater. 403 (2021). https://doi.org/10.1016/j.jhazmat.2020.123666.

[82] E. Ceballos, S.A. Bea, R. Sanci, Applying reactive transport modelling in a chromium-contaminated site in the Matanza-Riachuelo basin, Buenos Aires, Argentina, International Journal of Environment and Health. 9 (2018) 16–35. https://doi.org/10.1504/IJENVH.2018.090861.

[83] A. Thacharodi, S. Hassan, T.A. Hegde, D.D. Thacharodi, K. Brindhadevi, A. Pugazhendhi, Water a major source of endocrine-disrupting chemicals: An overview on the occurrence, implications on human health and bioremediation strategies, Environ Res. 231 (2023) 116097. https://doi.org/https://doi.org/10.1016/j.envres.2023.116097.

[84] I. Roy, J.F. Stoddart, Cyclodextrin Metal-Organic Frameworks and Their Applications, Acc Chem Res. (2021). https://doi.org/10.1021/acs.accounts.0c00695.

[85] E. Taheri, A. Fatehizadeh, E.C. Lima, M. Rezakazemi, High surface area acid-treated biochar from pomegranate husk for 2,4-dichlorophenol adsorption from aqueous solution, Chemosphere. 295 (2022) 133850. https://doi.org/https://doi.org/10.1016/j.chemosphere.2022.133850.

[86] W. Wang, T. Gong, H. Li, Y. Liu, Q. Dong, R. Zan, Y. Wu, The multi-process reaction model

778 and underlying mechanisms of 2,4,6-trichlorophenol removal in lab-scale biochar-
779 microorganism augmented ZVI PRBs and field-scale PRBs performance, Water Res. 217
780 (2022) 118422. https://doi.org/https://doi.org/10.1016/j.watres.2022.118422.
781 [87] O. Moradi, H. Alizadeh, S. Sedaghat, Removal of pharmaceuticals (diclofenac and
782 amoxicillin) by maltodextrin/reduced graphene and maltodextrin/reduced graphene/copper
783 oxide nanocomposites, Chemosphere. 299 (2022) 134435.
784 https://doi.org/https://doi.org/10.1016/j.chemosphere.2022.134435.
785 [88] W. Miran, J. Jang, M. Nawaz, A. Shahzad, D.S. Lee, Biodegradation of the sulfonamide
786 antibiotic sulfamethoxazole by sulfamethoxazole acclimatized cultures in microbial fuel
787 cells, Science of The Total Environment. 627 (2018) 1058–1065.
788 https://doi.org/https://doi.org/10.1016/j.scitotenv.2018.01.326.
789 [89] W. Tang, B. Shan, H. Zhang, W. Zhang, Y. Zhao, Y. Ding, N. Rong, X. Zhu, Heavy Metal
790 Contamination in the Surface Sediments of Representative Limnetic Ecosystems in Eastern
791 China, Sci Rep. 4 (2014) 7152. https://doi.org/10.1038/srep07152.
792 [90] T. Fan, X. Yao, Z. Sun, D. Sang, L. Liu, H. Deng, Y. Zhang, Properties and metal binding
793 behaviors of sediment dissolved organic matter (SDOM) in lakes with different trophic
794 states along the Yangtze River Basin: A comparison and summary, Water Res. 231 (2023)
795 119605. https://doi.org/https://doi.org/10.1016/j.watres.2023.119605.
796 [91] G. Li, Zhensheng. Liang, J. Sun, Y. Qiu, C. Qiu, X. Liang, Y. Zhu, P. Wang, Y. Li, F. Jiang,
797 A pilot-scale sulfur-based sulfidogenic system for the treatment of Cu-laden electroplating
798 wastewater using real domestic sewage as electron donor, Water Res. 195 (2021) 116999.
799 https://doi.org/https://doi.org/10.1016/j.watres.2021.116999.

[92] K. Li, M. Fu, L. Ma, H. Yang, Q. Li, Zero-valent iron drives the passivation of Zn and Cu during composting: Fate of heavy metal resistant bacteria and genes, Chemical Engineering Journal. 452 (2023) 139136. https://doi.org/https://doi.org/10.1016/j.cej.2022.139136.

[93] D. Park, Y.S. Yun, J.M. Park, XAS and XPS studies on chromium-binding groups of biomaterial during Cr(VI) biosorption, J Colloid Interface Sci. 317 (2008) 54–61. https://doi.org/10.1016/j.jcis.2007.09.049.

[94] F. AlShaarani, R.M. Alaisami, L. Aljerf, I.A. Jamous, K. Elias, A. Jaber, An auxiliary factor for increasing the retention of short abutments, Heliyon. 5 (2019). https://doi.org/10.1016/j.heliyon.2019.e02674.

[95] J. Ding, L. Pu, Y. Wang, B. Wu, A. Yu, X. Zhang, B. Pan, Q. Zhang, G. Gao, Adsorption and Reduction of Cr(VI) Together with Cr(III) Sequestration by Polyaniline Confined in Pores of Polystyrene Beads, Environ Sci Technol. 52 (2018) 12602–12611. https://doi.org/10.1021/acs.est.8b02566.

[96] Y. Ye, Z. Jiang, Z. Xu, X. Zhang, D. Wang, L. Lv, B. Pan, Efficient removal of Cr(III)-organic complexes from water using UV/Fe(III) system: Negligible Cr(VI) accumulation and mechanism, Water Res. 126 (2017) 172–178. https://doi.org/10.1016/j.watres.2017.09.021.

[97] Y. Deng, X. Wang, I. Lynch, Z. Guo, P. Zhang, L. Wu, X. Wu, T. Li, Homogeneous dispersion of amorphous nanoscale zero-valent iron supported on chlorella-derived biochar: In-situ synthesis and application mechanism for Cr(VI) removal over a wide pH range, Sep Purif Technol. 330 (2024). https://doi.org/10.1016/j.seppur.2023.125207.

Table 1 Comparison of pseudo-second-order rate constant for BPA or Cr(VI) by other reported adsorbents.

Materials	C_0	k_{obs} (g mg^{-1} min^{-1})		Temperature	pH	Reference
	mg/L	Cr	BPA	°C		
PANI@PCDP	32		0.14	25	6	This study
reduced graphene oxide-β-cyclodextrin aerogel	15		0.002	25	7	[46]
amphoteric β-cyclodextrin-based adsorbent	50		0.0015	25	4	[48]
sulfhydryl-richβ-cyclodextrin polymer	150		0.000145	25	6	[65]
β-cyclodextrin polyurethane	200		0.0002	25	-	[66]
β-cyclodextrin/ZrO_2 nanocomposite	100		0.079	25	6	[67]
β-cyclodextrin-derived sorbent	68		0.05	25	-	[68]
Defect-rich porous carbon	50		0.0002	25	7	[69]
amino group-functionalized covalent organic frameworks	100		0.0046	24.85	-	[70]
magnesium ascorbyl phosphate graphene-based monolith	10		0.008	25	7	[71]
Magnetic biochar	10		0.00039	25	-	[72]
PANI@PCDP	112	0.0088		25	6	This study
Folic Acid-PANI Hybrid Hydrogel	20	0.00102		25	2	[31]
PANi@faujasite composite	100	0.0002		25	2	[73]
PANI/γ-Fe_2O_3	100	0.00075		-	2	[32]
PANI@WO_3	100	0.00134		20	2	[74]
polydopamine@zeolitic idazolate frameworks-8	30	0.0079		20	5	[39]
Polypyrrole magnetic nanocomposite	100	0.0034		33	2	[75]
polypyrrole/calcium rectorite composite	100	0.0020		25	1.5	[13]
NH_2-graphene sponge	110	0.0020		25	2	[60]
Polypyrrole-carbon nanotubes nanocomposites	100	0.0005		25	2	[62]

826 **Table 2 Comparison of maximum adsorption capacity of PANI@PCPD for BPA or Cr(VI) against**

827 **other reported adsorbents.**

Materials	Equilibrium time	q_{max} (mg g^{-1})		Temperature	pH	Reference
	min	Cr	BPA	°C		
PANI@PCDP	30		36	25	6	This study
reduced graphene oxide-β-cyclodextrin aerogel	300		346	25	7	[46]
amphoteric β-cyclodextrin-based adsorbent	300		94.1	25	6.5	[48]
sulfhydryl-richβ-cyclodextrin polymer	480		287.875	25	6	[65]
β-cyclodextrin polyurethane	700		422.7	25	-	[66]
β-cyclodextrin/ZrO_2 nanocomposite	100		175	25	6	[67]
β-cyclodextrin-derived sorbent	20		93.5	25	-	[68]
defect-rich porous carbon	90		874	25	7	[69]
amino group-functionalized covalent organic frameworks	360		47.33	24.85	-	[70]
magnesium ascorbyl phosphate graphene-based monolith	900		324.27	25	7	[71]
Magnetic biochar	120		29.66	25	-	[72]
PANI@PCDP	20	81		25	6	This study
Folic Acid-PANI Hybrid Hydrogel	250	171.2		25	2	[31]
PANi@faujasite composite	400	384.6		25	2	[73]
PANI/γ-Fe_2O_3	60	195.7		-	2	[32]
PANI@WO_3	120	549.37		20	2	[74]
polydopamine@zeolitic idazolate frameworks-8	480	136.56		20	5	[39]
Polypyrrole magnetic nanocomposite	90	208.77		33	2	[75]
polypyrrole/calcium rectorite composite	100	714.29		25	1.5	[13]
NH_2-graphene sponge	600	166.46		25	2	[60]
Polypyrrole-carbon nanotubes nanocomposites	150	294.1		25	2	[62]
Zero-valent iron@chlorella-derived biochar	120	26.67		25	5	[97]

828

Figures

Figure 1

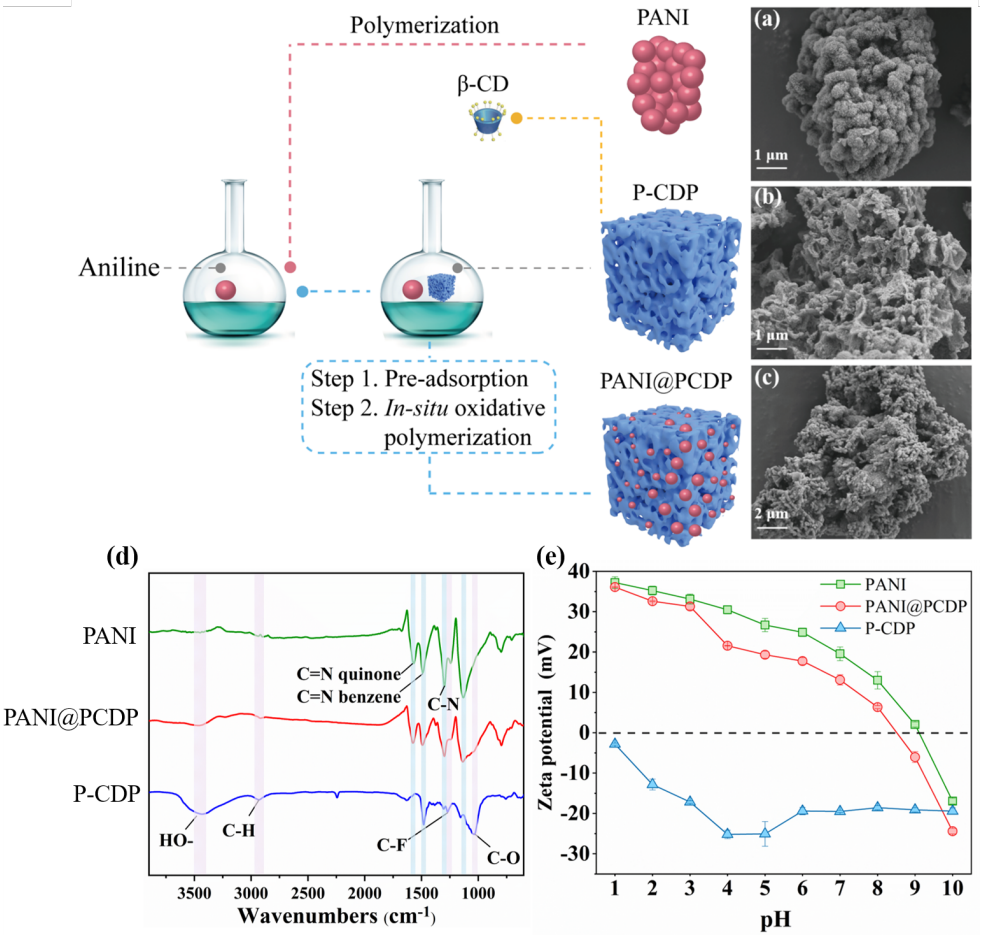

Fig. 1. The synthetic route of PANI@PACD and SEM images of PANI (a), P-CDP (b), and PANI@PCDP (c). FT-IR spectra of the sorbents (d). Zeta potentials of the sorbents as a function of pH (e).

834 **Figure 2**

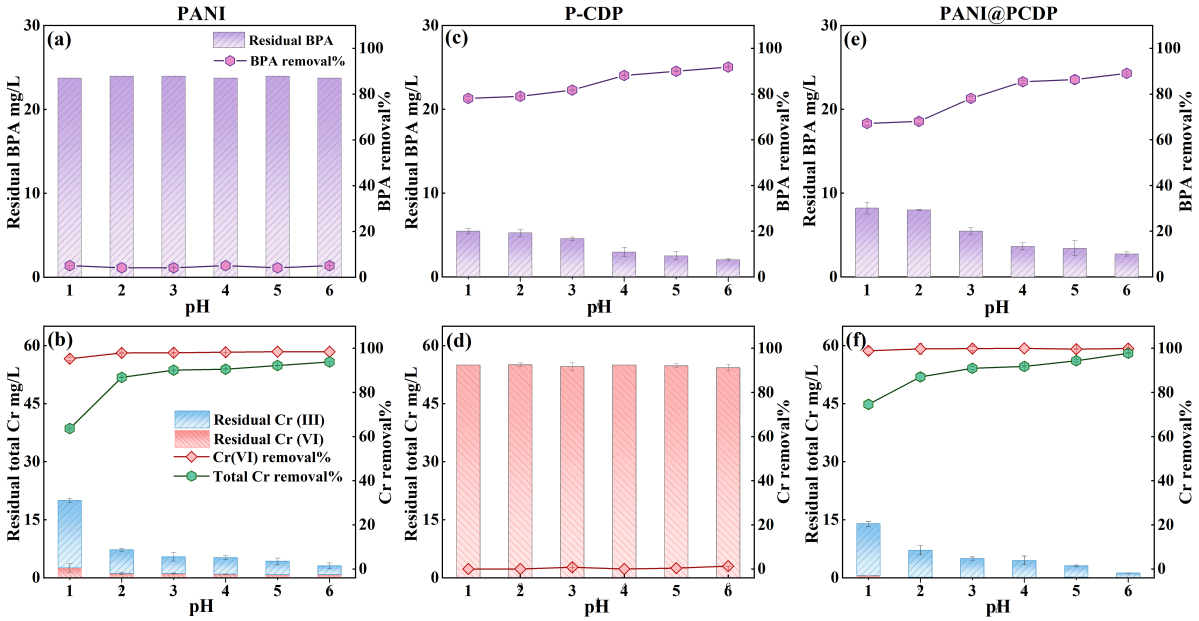

835

836 **Fig. 2.** Impacts of pH on the uptake of BPA (25 mg L^{-1}) by (a) PANI, (c) P-CDPs, and PANI@PCDP at

837 a sorbent dose of 1 g L^{-1}. Impacts of pH on the adsorption and reduction process of Cr(VI) (55 mg L^{-1})

838 on (b) PANI, (d) P-CDPs, and (f) PANI@PCDP at a sorbent dose of 1 g L^{-1}.

839 **Figure 3**

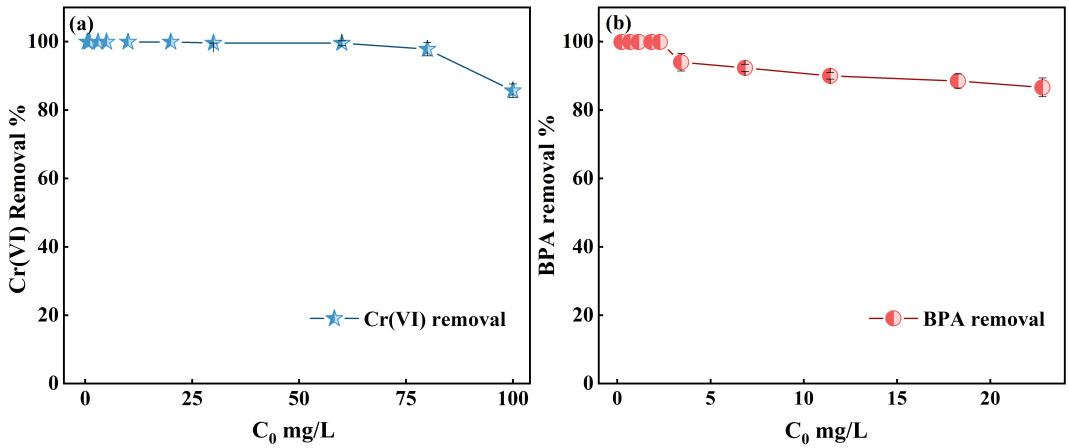

840

841 **Fig. 3.** Removal of (a) Cr(VI) (0.5-100 mg L^{-1}) and (b) BPA (0.228-22.8 mg L^{-1}) by PANI@PCDP (1 g

842 L^{-1}) at pH 6.0 as a function of initial concentrations of pollutants.

843 **Figure 4**

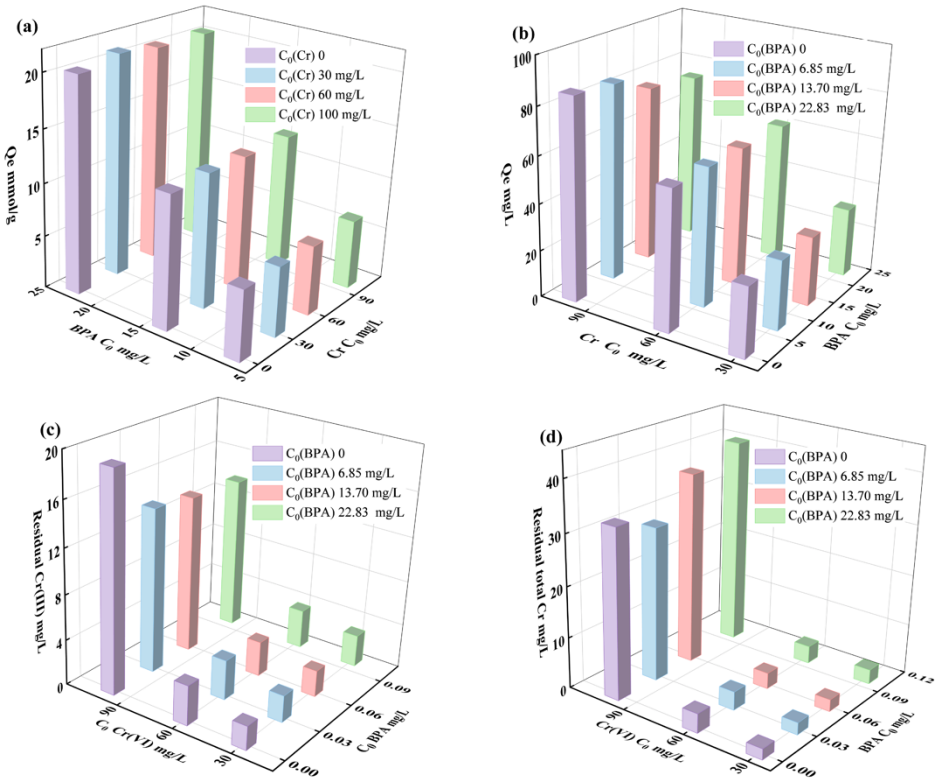

844

845 **Fig. 4.** Adsorption performance of PANI@PCDP (1 g L^{-1}) at pH 6.0 in binary system. (a) Effect of Cr(VI)

846 on the BPA adsorption; (b) Effect of BPA on Cr(VI) adsorption and reduction process, on (c) Cr(III)

847 sequestration, on (d) total Cr removal.

848 **Figure 5**

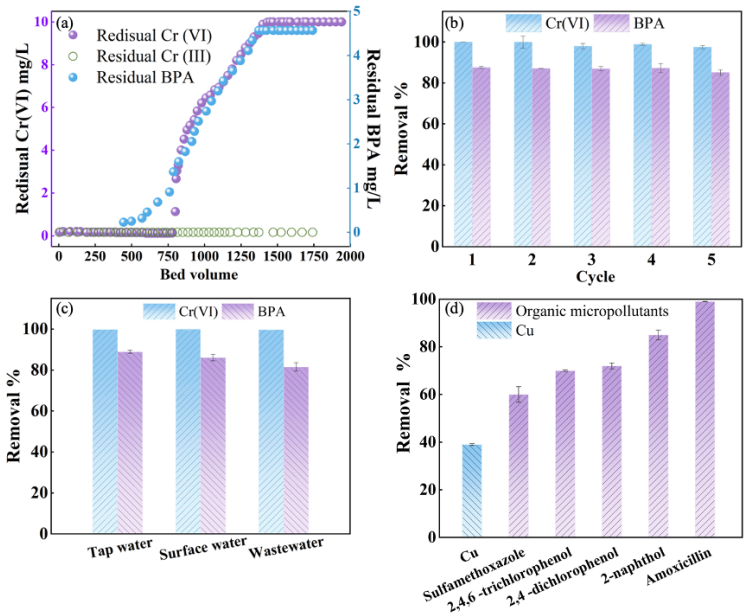

849

850 **Fig. 5.** (a) Column adsorption test with a binary solution (Cr(VI) 10 mg L^{-1}, BPA 4.6 mg L^{-1}, 0.38 g

851 PANI@PCDP, pH 6.0). (b) Regeneration study for PANI@PCDP. (c) Removal of BPA (22.8 mg L^{-1}) and

852 Cr(VI) (50 mg L^{-1}) using PANI@PCDP (1 g L^{-1}) at pH 6.0 in real matrices. (d) Removal of typical

853 emerging micropollutant using PANI@PCDP at pH 6.0 (sorbent 1 g L^{-1}, Cu(II) 55 mg L^{-1},

854 sulfamethoxazole 0.04 mmol L^{-1}, other organic absorbates 0.1 mmol L^{-1}).

855

856

857 **Figure 6**

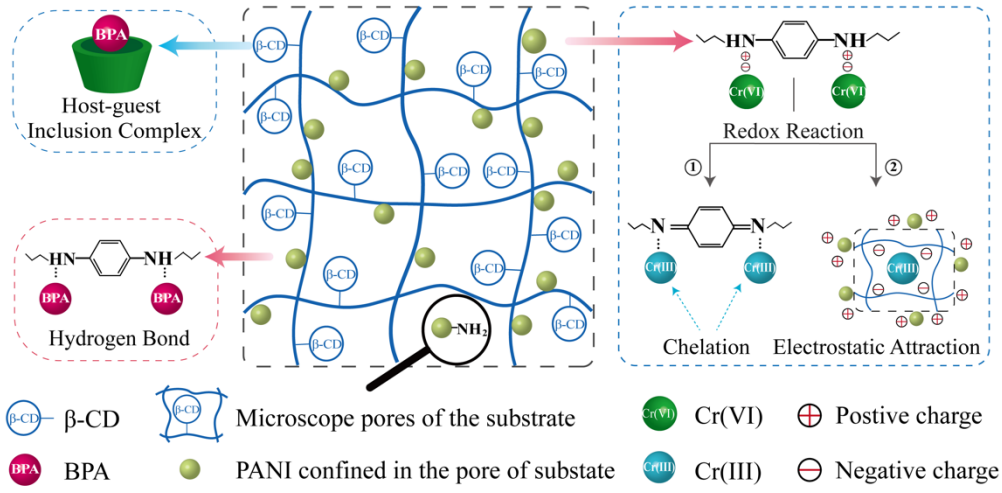

858

859 **Fig. 6.** Mechanisms for simultaneous removal of BPA, Cr(VI) and Cr(III) by PANI@PCDP.

860 **Figure 7**

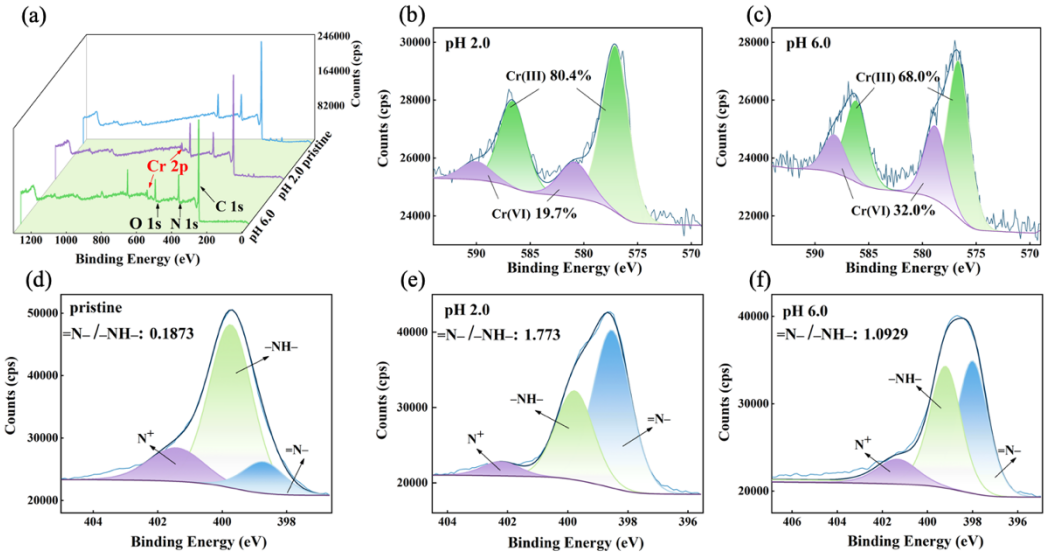

861

862 **Fig. 7.** XPS scan spectra of PANI@PCDP before and after Cr(VI) adsorption at pH 2.0 and pH 6.0 (a).

863 XPS spectra of Cr 2p spectra for PANI@PCDP after Cr(VI) adsorption at pH 2.0 (b) and pH 6.0 (c). XPS

864 spectra of N 1s for PANI@PCDP before (d) and after Cr(VI) adsorption at pH 2.0 (e) and pH 6.0 (f).

Supporting Information

for

Simultaneous removal of organic micropollutants and metals from water by a multifunctional β-cyclodextrin polymer-supported-polyaniline composite

Pin Wang [a], Guangyu An [b], Peter Jarvis [c], Wen Liu [d], Shunke Ding [a], Ruixin Qu [a], Zhanghan Li [a], Cheng Ye[a], Wenhai Chu [a, *]

[a] State Key Laboratory of Pollution Control and Resource Reuse, College of Environmental Science and Engineering, Tongji University, Shanghai, 200092, China

[b] State Key Laboratory of Environmental Aquatic Chemistry, Research Center for Eco-Environmental Sciences, Chinese Academy of Sciences, Beijing, 100085, China

[c] School of Water, Energy and Environment, Cranfield University, College Road, Cranfield, Bedfordshire MK43 0AL, United Kingdom

[d] College of Environmental Sciences and Engineering, Peking University, Beijing 100871, China

* Corresponding author:

E-mail address: feedwater@126.com

Address: Room 407, National Engineering Research Center for Urban Pollution Control, 1239 Siping Road, Yangpu District, Shanghai, 200092, China

Text S1 Analysis of BPA

The concentration of BPA was measured using high-performance liquid chromatography (HPLC-2010, SHIMAZU, Kyoto, Japan) with a UV detector and an Agilent Shim-pack C18 column (250 mm × 4.6 mm, 5 μm). The Injection volume was 20 μL. The mobile phase contained acetonitrile and Milli-Q water (18.25 MΩ) (3: 2, v/v). The flow rate was 1.0 mL min^{-1}, and the detection wavelength was 285 nm.

Text S2 Data Analysis

The efficiency of pollutant removal (in %) by the sorbent was calculated by the following equation:

$$\text{Removal efficiency} = \frac{C_0 - C_t}{C_0} \times 100$$

where C_0 (mmol L^{-1} for BPA, mg L^{-1} for Cr) and C_t (mmol L^{-1} for BPA, mg L^{-1} for Cr) are the initial and residual concentration of pollutant in the solution and filtrate, respectively.

The adsorption capacity of the sorbent was determined by the following equation:

$$q_t = \frac{(C_0 - C_t)\,V}{m}$$

where q_t (mg L^{-1}) is the amount of pollutant adsorbed per gram of sorbent at time t (min). C_0 (mmol L^{-1}) and C_t (mmol L^{-1}) are the initial and residual concentration of pollutant in the solution and filtrate, respectively. m (g) is the mass of sorbent used in each experiment. In the case of BPA, q_t multiplying by Mw (g mol^{-1}), the molar mass of the pollutant, obtains the final adsorption capacity (mg L^{-1}).

Text S3 Kinetics study

The experimental data of PANI@PCDP kinetic study was best described by Ho and McKay's pseudo-second-order adsorption model.[1]

$$\frac{t}{q_t} = \frac{t}{q_e} + \frac{1}{k_{obs}\, q_e^2}$$

Where q_t and q_e are the adsorption capacity (mg g^{-1}) at time t (minute) and at equilibrium, respectively, and k_{obs} is a second-order rate constant (g mg^{-1} min^{-1}).

Text S4 Adsorption Isotherms

The experimental isotherm data of PANI@PCDP thermodynamic study was best fitted with the Langmuir model, which was generated by plotting $1/q_e$ versus 1/c according to the following equation:

$$\frac{1}{q_e} = \frac{1}{q_{max,e}} + \frac{1}{q_{max,e}\, KC_e}$$

where q_e (mg/g) is the adsorption capacity of the sorbent at equilibrium, $q_{max,e}$ (mg g^{-1}) is the maximum adsorption capacity of adsorbent at equilibrium, C_e (mol L^{-1}) is the residual concentration of the pollutant at equilibrium, and K (1 mol^{-1}) is the equilibrium constant.

Table S1 Experimental design for the simultaneous adsorption of Cr(VI) and BPA to PANI@PCDP

	Factor A: initial concentration of BPA, mmol L^{-1}				
Factor B: initial concentration of Cr(VI), mg/L		0	0.03	0.06	0.1
	0	-	q_e(0.03, 0)	q_e(0.06, 0)	q_e(0.1, 0)
	30	q_e(0, 30)	q_e(0.03, 30)	q_e(0.06, 30)	q_e(0.1, 30)
	60	q_e(0, 60)	q_e(0.03, 60)	q_e(0.06, 60)	q_e(0.1, 60)
	100	q_e(0, 100)	q_e(0.03, 100)	q_e(0.06, 100)	q_e(0, 100)

Table S2 Characteristics of real water samples

	Dissolved organic matter (mg L^{-1})	Turbidity (NTU)	pH
Tap water	1.5	0.06	7.1
Surface water	5.3	5.5	7.9
Wastewater	14	12.0	8.3

Table S3 Analysis of organic micropollutants using a HACH DR6000 UV–vis spectrophotometer.

Micropollutants	Wavelength
2,4-dichlorophenol	284
2,4,6-trichlorophenol	280
2-naphthol	273
Sulfamethoxazole	262
Amoxicillin	270

Figure S1

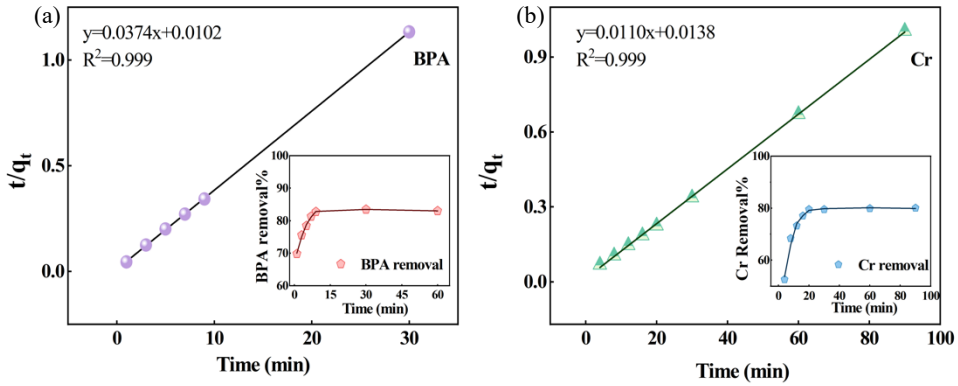

Fig. S1. Pseudo-second-order kinetic model fit for the (a) BPA (32 mg L^{-1}) adsorption and (b) Cr(VI) adsorption (112 mg L^{-1}) onto PANI@PCDP (1g L^{-1}) at pH 6.0.

Figure S2

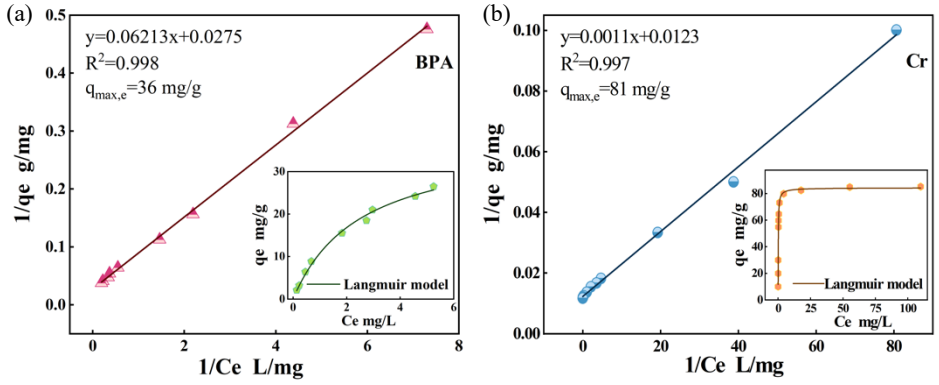

Fig. S2. Langmuir isotherm of (a) BPA (2.28–31.73 mg L^{-1}, equivalent to 0.01-0.139 mmol L^{-1}) adsorption and (b) Cr(VI) (10–200 mg L^{-1}) adsorption by PANI@PCDP (1g L^{-1}) at pH 6.0.

Figure S3

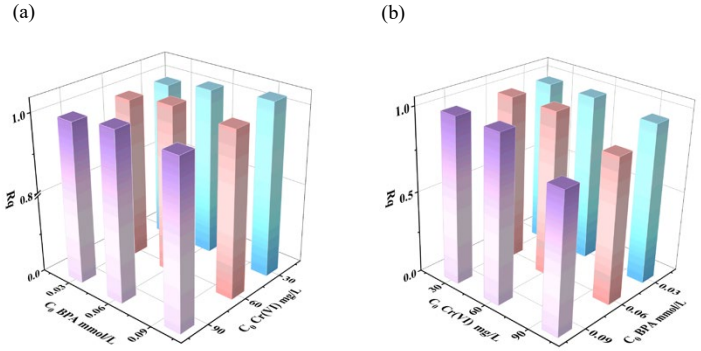

Fig. S3. Ratio of adsorption capacity versus the initial pollutant concentrations in the binary systems for simultaneous removal of Cr(VI) and BPA.

Figure S4

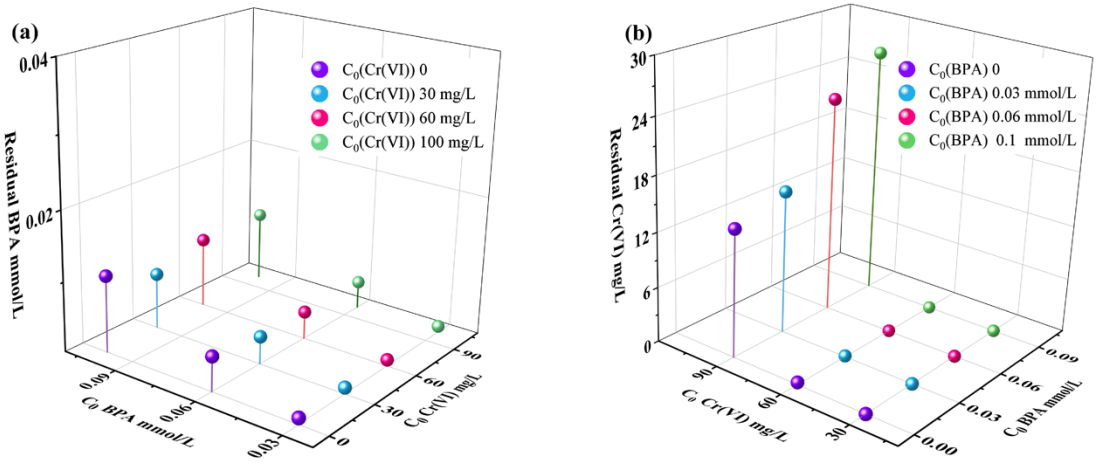

Fig. S4. Residual concentration of BPA (a) and Cr(VI) (b) versus the initial pollutant concentrations in the binary systems. ([BPA]$_0$: 6.85 mg L^{-1}, 13.70 mg L^{-1}, and 22.83 mg L^{-1}, PANI@PCDP 1 g L^{-1}, pH 6.0)

Figure S5

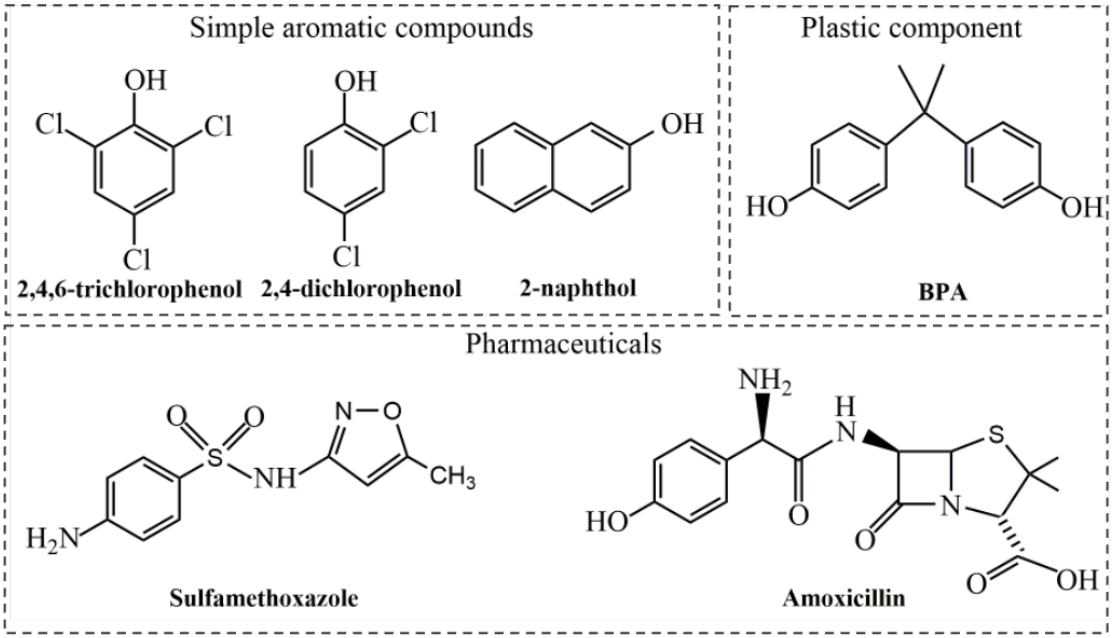

Fig. S5. Structure of the emerging pollutants.

Figure S6

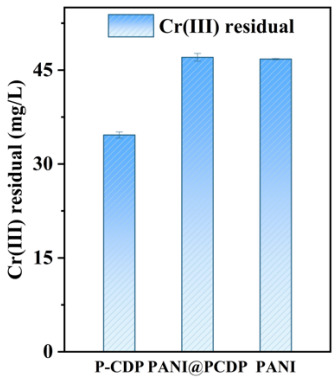

Fig. S6. Removal of Cr(III) from $CrCl_3$ solution (50 mg L^{-1}) by the sorbents (1 g L^{-1}) at pH 6.0.

Reference:

[1] Y.S. Ho, G. McKay, Pseudo-second order model for sorption processes, Process Biochemistry. 34 (1999) 451–465. https://doi.org/https://doi.org/10.1016/S0032-9592(98)00112-5.

https://dspace.org/

Simultaneous removal of organic micropollutants and metals from water by a multifunctional -cyclodextrin polymer-supported-polyaniline composite

Wang, Pin; An, Guangyu; Jarvis, Peter; Liu, Wen; ShunkeDing, Shunke ...

2024-02-15
Elsevier
https://doi.org/10.1016/j.cej.2024.148826
Wang P, An G, Jarvis P, et al., (2024) Simultaneous removal of organic micropollutants and metals from water by a multifunctional -cyclodextrin polymer-supported-polyaniline composite. Chemical Engineering Journal, Volume 482, February 2024, Article number 148826

Downloaded from a DSpace repository. https://dspace.org/